2016-06

Centrifugal tensioned metastable fluid detectors for trace radiation sources: experimental verification and military employment

Chiaverotti, Dominic J.

Monterey, California: Naval Postgraduate School

NAVAL POSTGRADUATE SCHOOL

MONTEREY, CALIFORNIA

THESIS

CENTRIFUGAL TENSIONED METASTABLE FLUID DETECTORS FOR TRACE RADIATION SOURCES: EXPERIMENTAL VERIFICATION AND MILITARY EMPLOYMENT

by

Dominic J. Chiaverotti

June 2016

Thesis Advisor: Craig F. Smith
Co-Advisor: Anthony G. Pollman

THIS PAGE INTENTIONALLY LEFT BLANK

REPORT DOCUMENTATION PAGE			*Form Approved OMB No. 0704–0188*

1. AGENCY USE ONLY	**2. REPORT DATE** June 2016	**3. REPORT TYPE AND DATES COVERED** Master's Thesis

4. TITLE AND SUBTITLE CENTRIFUGAL TENSIONED METASTABLE FLUID DETECTORS FOR TRACE RADIATION SOURCES: EXPERIMENTAL VERIFICATION AND MILITARY EMPLOYMENT	**5. FUNDING NUMBERS**
6. AUTHOR(S) Dominic J. Chiaverotti	
7. PERFORMING ORGANIZATION NAME(S) AND ADDRESS(ES) Naval Postgraduate School Monterey, CA 93943–5000	**8. PERFORMING ORGANIZATION REPORT NUMBER**
9. SPONSORING /MONITORING AGENCY NAME(S) AND ADDRESS(ES) N/A	**10. SPONSORING / MONITORING AGENCY REPORT NUMBER**

11. SUPPLEMENTARY NOTES The views expressed in this thesis are those of the author and do not reflect the official policy or position of the Department of Defense or the U.S. Government. IRB Protocol number ____N/A____.

12a. DISTRIBUTION / AVAILABILITY STATEMENT Approved for public release; distribution is unlimited	**12b. DISTRIBUTION CODE**

13. ABSTRACT (maximum 200 words)

Centrifugal tensioned metastable fluid detectors (CTMFDs) promise a compact, easy to use, highly sensitive, robust, discriminatory, mobile sensor platform that could detect the presence of special nuclear materials in real time. CTMFDs could help in the detection of fast neutrons or alpha particles that are telltale signs of nuclear material, while remaining blind to gamma radiation that could otherwise interfere with the desired measurement. CTMFDs have a simple, easy-to-use equipment string that costs on the order of hundreds of dollars compared with traditional detectors with similar capabilities, which cost on the order of thousands of dollars.

This study involved laboratory testing comparing the CTMFD's capabilities of actinide spectroscopy and neutron detection against other detection systems with similar capabilities. The CTMFD was found to have a comparable neutron detection efficiency, and was found to be much more effective at discriminating between highly diluted actinide solutions using alpha particle spectroscopy. Employment of the proper CTMFD setup could involve use at military checkpoints, or aiding in determining origins of a nuclear weapon in a post-detonation analysis scenario.

14. SUBJECT TERMS TMFD, neutron radiation, alpha radiation, gamma radiation, metastable fluids, detection efficiency, neutron detection	**15. NUMBER OF PAGES** 99
	16. PRICE CODE

17. SECURITY CLASSIFICATION OF REPORT	**18. SECURITY CLASSIFICATION OF THIS PAGE**	**19. SECURITY CLASSIFICATION OF ABSTRACT**	**20. LIMITATION OF ABSTRACT**
Unclassified	Unclassified	Unclassified	UU

NSN 7540–01–280–5500 Standard Form 298 (Rev. 2–89) Prescribed by ANSI Std. 239–18

THIS PAGE INTENTIONALLY LEFT BLANK

Approved for public release; distribution is unlimited

CENTRIFUGAL TENSIONED METASTABLE FLUID DETECTORS FOR TRACE RADIATION SOURCES: EXPERIMENTAL VERIFICATION AND MILITARY EMPLOYMENT

Dominic J. Chiaverotti
Captain, United States Marine Corps
B.S., Marquette University, 2010

Submitted in partial fulfillment of the
requirements for the degree of

MASTER OF SCIENCE IN APPLIED PHYSICS

from the

NAVAL POSTGRADUATE SCHOOL
June 2016

Approved by: Craig F. Smith
Thesis Advisor

Anthony G. Pollman
Co-Advisor

Kevin B. Smith
Chair, Department of Physics

THIS PAGE INTENTIONALLY LEFT BLANK

ABSTRACT

Centrifugal tensioned metastable fluid detectors (CTMFDs) promise a compact, easy to use, highly sensitive, robust, discriminatory, mobile sensor platform that could detect the presence of special nuclear materials in real time. CTMFDs could help in the detection of fast neutrons or alpha particles that are telltale signs of nuclear material, while remaining blind to gamma radiation that could otherwise interfere with the desired measurement. CTMFDs have a simple, easy-to-use equipment string that costs on the order of hundreds of dollars compared with traditional detectors with similar capabilities, which cost on the order of thousands of dollars.

This study involved laboratory testing comparing the CTMFD's capabilities of actinide spectroscopy and neutron detection against other detection systems with similar capabilities. The CTMFD was found to have a comparable neutron detection efficiency, and was found to be much more effective at discriminating between highly diluted actinide solutions using alpha particle spectroscopy. Employment of the proper CTMFD setup could involve use at military checkpoints, or aiding in determining origins of a nuclear weapon in a post-detonation analysis scenario.

THIS PAGE INTENTIONALLY LEFT BLANK

TABLE OF CONTENTS

THIS PAGE INTENTIONALLY LEFT BLANK

LIST OF FIGURES

LIST OF TABLES

LIST OF ACRONYMS AND ABBREVIATIONS

Bq	becquerel
BF_3	boron trifluoride
Co	cobalt
cpm	counts per minute
cps	counts per second
Cs	cesium
CTMFD	centrifugal tensioned metastable fluid detector
DOD	Department of Defense
DTRA	Defense Threat Reduction Agency
KAERI	Korea Atomic Energy Research Institute
LS	liquid scintillation
NPS	Naval Postgraduate School
PMT	photomultiplier tube
PSD	pulse shape discrimination
Pu	plutonium
SF	spontaneous fission
SNM	special nuclear material
STP	standard temperature and pressure
U	uranium
UN	uranyl nitrate

THIS PAGE INTENTIONALLY LEFT BLANK

ACKNOWLEDGMENTS

I would first like to thank Dr. Craig Smith, whose passion for nuclear engineering and keen ability to push his students has had a profound impact on me and my time here at the Naval Postgraduate School. I will forever be grateful for the time he took to develop my education and my thesis, and I aspire to be more like him in all that I do.

Dr. Tony Pollman, a fellow Marine who also shared many of my passions and research interests, stimulated my excitement in this project and has continued to be a great friend and mentor. If it were not for his mentorship and guidance, this project would never have gotten off the ground.

The Nuclear Science and Engineering Research Center at West Point, and specifically Major Andrew Decker and Lieutenant Colonel Robert Prins, was supportive of my efforts every step of the way. Their willingness to provide assistance financially as well as academically to a member of a different service branch, 3,000 miles away, taught me more than any academic instruction could have. I am forever indebted to their graciousness.

Dr. Brian Archambault of Sagamore Adams Laboratories, LLC, was of great assistance during the long hours of laboratory research, and was always quick to respond to my seemingly never-ending emails and questions. Dr. Rusi Taleyarkhan of Purdue University was also extremely hospitable on all of my trips to visit with him, and he provided overarching leadership that helped me to see this project through to the end.

The professors, staff, and students at NPS served as an inspiration to me, and taught and motivated me in ways that no other graduate institution could have. I would especially like to thank Professors Richard Harkins and Dr. Pete Crooker, who put up with me and my questions and kept me on the right track over the last two years.

Last, but certainly not least, my family has provided tremendous support to me and my academic and work-related achievements as far back as I can remember. I have been blessed with amazing parents and grandparents, and I am truly fortunate to have them as my cheerleaders in every endeavor. My sister, Francesca, however, is a punk.

THIS PAGE INTENTIONALLY LEFT BLANK

I. INTRODUCTION

A. MOTIVATION

After the development of nuclear weapons helped the United States and its allies to win World War II in 1945, it soon became clear that these weapons had the potential to play a pivotal role in future global conflict. Although massive destruction on a global scale during the Cold War was successfully avoided, the threat of a weapon of mass destruction to be used by a state or non-state actor continues to present a significant threat to the security and interests of the United States. According to a report by the Stockholm International Peace Research Institute, as June of 2014 there are nine countries known or believed to possess nuclear weapons [1]. Although a threat from Russia or China should not be discounted, the greater threat may well be from the likes of North Korea, Iran, or an independent terrorist organization that is able to purchase a nuclear weapon on the black market and smuggle it into the United States. The prevention or mitigation of such an attack is an important objective of the Defense Threat Reduction Agency of the DOD, which is entrusted to "Prevent, deter, detect, locate, characterize, track, defeat, and mitigate existing or future CBRNE threats or devices" [2].

Although the state of the art in detection of special nuclear material (SNM) involves detectors of various types and capabilities, a relatively new approach involves the use of the centrifugal tensioned metastable fluid detector (CTMFD). CTMFDs promise a compact, easy to use, highly sensitive, robust, discriminatory sensor platform that could detect the presence of special nuclear materials in real time [3]. Unlike other detectors, CTMFDs are mobile, cheap to construct (under $1000), and are blind to the gamma radiation that plagues other detectors and prevents them from discriminating between kitty litter and a nuclear weapon. While there has been much research done on the likes of more common technology such as liquid scintillators, there has been very little research done on CTMFDs, especially with relevance to the mission of U.S. national defense. If proven to be effective, CTMFDs could provide DTRA with a cheaper, mobile platform that will allow it to conduct its mission of protecting the United States from the threat of a nuclear weapon.

B. APPROACH

In order to fully grasp the capabilities as well as the advantages and disadvantages of the centrifugal tensioned metastable fluid detector, it is crucial to get hands-on time with the detector itself in a laboratory setting that allows analysis with relevant isotopes. It is also important to compare the capabilities of other current state of the art detectors in the same laboratory environment and with the same isotopes, to determine if the CTMFD does indeed provide a distinct advantage. Through funding from the Defense Threat Reduction Agency and in partnership with Sagamore Adams Laboratories, LLC (affiliated with Purdue University), laboratory time as well as oversight with relevant isotopes was provided that allowed for such an analysis.

Since the CTMFD promises to provide the capabilities of detection of fast neutrons from an external source, as well as actinide spectroscopy of a source inside the detector, it was important to set up a lab environment that allowed for analysis of both of these capabilities. First, a neutron source was analyzed from various distances with both the CTMFD as well as two other detector types, which were compared for efficiency. Second, multiple actinide solutions with similar concentrations were created, and then analyzed through both the CTMFD as well as another detector to determine efficiency. In addition to efficiency, other factors were analyzed during the experiments to evaluate ease of use, detector cost, and feasibility in the use of conducting DTRA's mission.

C. RESEARCH OBJECTIVES AND GOALS

The precise goal of this study is to evaluate the effectiveness of the centrifugal tensioned metastable fluid detector and analyze its potential for use in a military environment. In order to be successful in that endeavor, this study aimed to answer the following specific research questions:

- What types of detectors are currently used for detection/identification of a radioactive source, and what are their strengths and weaknesses?

This question was answered through research of current state of the art detectors and, more importantly, through hands-on experimentation and data analysis with these detectors in the same laboratory environment used to analyze the CTMFD. The detectors

were selected to provide a similar capability to the CTMFD in that they must be able to either detect fast neutrons (or alpha particles) or determine which actinide source is present (if any). This portion of the study also involved a detailed analysis of the theory behind radiation detection, to include detection of fast neutrons, gamma rays, and alpha and beta particles.

- What are the theoretical underpinnings of the CTMFD?

Before any experimentation took place at Sagamore Adams Laboratories, it was important to analyze the working scientific principles of the CTMFD, and to understand the potential benefits that these principles could provide. This involved both a review of current literature on the topic as well as an in-depth dialogue with researchers and scientists who are responsible for the creation and development of this technology.

- How do experimental results of fast neutron detection and actinide spectroscopy compare to applicable theory for the CTMFD?

This involved conducting specific laboratory experimentation to analyze both the neutron detection and actinide spectroscopy capabilities of the CTMFD with various isotopes.

- Does the CTMFD provide a distinct advantage over current state of the art detectors and if so, what techniques, tactics, or procedures are required to properly and effectively employ the detector for any related SNM source that could be of interest to DTRA?

Once the experimental data was taken to analyze both the capabilities of current state of the art detectors as well as the CTMFD, the overall goal was to compare the efficiencies of the selected systems and analyze their effectiveness, cost, and overall capability to assist DTRA in conducting its mission of securing the United States against a nuclear threat. Further, this study outlined specific methodologies to employ the CTMFD based on its experimental successes (or failures) in both fast neutron detection and alpha particle spectroscopy.

This study will be broken down into three chapters following this introduction. Chapter II presents a background on various types of ionizing radiation, and introduces three other detector types that have similar capabilities to that of the CTMFD. This includes experimental data from tests done with the Beckman LS 6500 Scintillation

System (for alpha spectroscopy comparison), as well as the NE-213 liquid scintillator and boron trifluoride detector (for neutron detection efficiency comparison). Chapter III provides an outline of the CTMFD theory and capabilities, as well as the experimentation results of its neutron detection efficiency and alpha spectroscopy capabilities. Chapter IV presents the conclusions of this study, to include a summary of scientific findings as well as recommendations for CTMFD employment and future research.

II. STATE OF THE ART DETECTOR TECHNOLOGY

A. THEORY

Within the nucleus of an atom of a given element, only certain combinations of protons and neutrons will allow the atom itself to be stable. Although there may be several isotopes of an element that involve different numbers of neutrons, having too many or too few neutrons in relation to the number of protons within the atom results in an unstable nucleus, which then undergoes radioactive decay [4]. Although there are many different types of radiation, the ones that are applicable to this thesis include alpha, beta, gamma, and neutron radiation. All of these types of radiation differ not only in their rudimentary makeup, but also in energy, mass, and their ability to penetrate different thicknesses of material. Neutron radiation will get a special emphasis considering that it generally originates in nuclear processes that may signal the presence of nuclear materials either separately or as part of a nuclear weapon. However, the other three types are also relevant in that they can also sometimes signal nuclear processes, and further aid in forensically determining the true makeup of a particular material.

1. Alpha Radiation

Alpha radiation occurs when an atom from a radioisotope source such as ^{238}U or ^{239}Pu decays and emits the equivalent of a helium-4 nucleus, reducing the radioisotope atom's mass number by four and the atomic number by 2. A common example of this is

$$^{238}_{92}U \rightarrow {}^{234}_{90}Th + {}^{4}_{2}He\,.$$

More generally, the spontaneous emission of an alpha particle from a nucleus can be written as

$${}^{A}_{Z}X \rightarrow {}^{A-4}_{Z-2}Y + {}^{4}_{2}\alpha\,.$$

Compared to other particles emitted from a radioactive process, alpha particles have a higher mass and electric charge, but a slower speed, and therefore a lower penetration depth [5]. Alpha particles generally do not travel more than a few centimeters in air,

cannot deeply penetrate human skin, and can be effectively shielded by thin materials such as a sheet of paper. Alpha decay typically occurs in nuclei with a mass greater than that of a nickel atom, and can deposit a large amount of energy into a shallow surface due to its relatively large mass and electric charge.

2. Beta Radiation

Beta decay involves the emission of a much lighter particle from an atom, namely a single electron or positron, as opposed to a helium nucleus that is emitted during alpha decay. Schematically, the β^- decay process is written as

$$ {}^{A}_{Z}X \rightarrow {}^{A}_{Z+1}Y + \beta^- , $$

where X is the beginning nuclear specimen and Y is the recoil nucleus. The recoil nucleus shows a relatively small amount of recoil energy in this decay process, but generally not enough to be detected by conventional means. The beta particle, therefore, is the most significant reaction product from the beta decay process.

The β^- decay process generally occurs when the ratio between neutrons and protons in an atom is too high (neutron-rich), and the atom changes a neutron into a proton while emitting an electron, which results in nuclear transmutation and the formation of a new element. A common example of the β^- decay process occurs in strontium-90 as follows:

$$ {}^{90}_{38}Sr \rightarrow {}^{90}_{39}Y + \beta^- . $$

The similar process of positron decay (β^+ decay) occurs in proton-rich nuclei with a positron (β^+) particle being emitted instead of an electron (the β^- particle). Due to its relatively low mass, the beta particle can travel up to a few feet in air at STP [6]. Beta particles, as with other forms of ionizing radiation, can also cause damage to certain living cells by breaking chemical bonds and turning certain atoms into ions. Beta radiation can be stopped by relatively thin, solid materials such as aluminum foil. Beta radiation is most commonly used in some cancer treatments, in chemical and biological tracing, and can be used in the manufacturing industry to determine the thicknesses of various materials [5].

3. Gamma Radiation

Gamma radiation typically occurs after an atom has undergone alpha or beta decay, and the daughter nucleus has reached an unstable energy level. In order to release some of this energy and become stable, the nucleus will emit pure energy in the form of a photon, called a gamma photon. Gamma photons are different than alpha and beta particles in that they have no charge or mass but instead consist of pure energy. Since these photons travel at the speed of light and have no electric charge, they can travel quite far through air before losing energy, and can only be stopped by very dense materials such as lead [6]. Gamma photons are often emitted from nuclear processes, but there is a significant amount of background gamma radiation from naturally occurring radioisotopes and interactions of cosmic rays with the atmosphere. Gamma rays are also emitted from everyday household items such as kitty litter and bananas, which both contain amounts of radioactive potassium. Gamma detectors can therefore sometimes mistake a shipment of household goods for enriched uranium, which therefore indicates that alternate methods of detection, such as fast neutron detection, are in some cases more effective at identifying potential special nuclear material [5].

4. Neutron Radiation

In processes such as radioactive decay and nuclear fission and fusion, free neutrons may be released that then interact with other atoms to create new isotopes and trigger further nuclear interactions. The process can begin when an atom spontaneously fissions or is struck by a high energy gamma photon, an alpha particle, or another neutron, and when the ejected neutrons strike another atom, they can trigger additional nuclear reactions that result in the emission of gammas or further neutron radiation. Once a neutron is ejected from the nucleus, it can be categorized as a fast neutron or a slow (thermal) neutron depending on its energy. In order for the process to be efficient enough to sustain the fission process for a thermal nuclear reactor, fast neutrons need to be slowed down through a medium such as water or graphite so that they have a higher chance of being absorbed or otherwise interacting with another nucleus. In nuclear weapons applications where higher, immediate energy output is required, no moderator is

used to slow down the neutrons during the fission process. Fast neutrons can be emitted from radioactive waste, as well as from materials containing U-238 or Pu-240. Although U-235 and Pu-239 are the isotopes largely associated with nuclear weapons material, the higher spontaneous fission rates of U-238 and Pu-240, which are also present in nuclear weapons material, are what make these materials detectable using passive detection methods [7]. While fast neutrons can also be found in synthetic spontaneous fission sources such as Cf-252, the fact that fast neutrons largely are produced only by radioactive sources makes them good candidates for detection of special nuclear material and more specifically, nuclear weapons [4], [5].

B. CURRENT STATE OF THE ART DETECTORS

In order to provide comparison with the capabilities of the centrifugal tensioned metastable fluid detector, three current state of the art detectors with similar capabilities were chosen to conduct experimentation with. The Beckman LS 6500 Scintillation System can be used to measure activity and discriminate between radioactive sources, and therefore provides an applicable comparison to the alpha particle spectroscopy capabilities of the CTMFD. Two separate state of the art detectors were chosen to experiment with and provide comparison to the neutron detection capabilities of the CTMFD: the NE-213 liquid scintillator and the boron trifluoride (BF_3) detector.

1. Scintillation Detectors

One of the methods of effective detection and spectroscopy of ionizing radiation is the scintillation process. The working principle behind the scintillation method is to convert the energy and associated ionization from radioactive decay into pulses of light. These pulses of light are then detected by a photodiode or a photomultiplier tube and converted into electrical pulses which allow a computer to count the number of pulses in a specified amount of time. Based on the number of counts that are detected, the radioactivity of the source can be calculated and compared to background levels [5], [8].

a. Beckman LS 6500 Scintillation System

The Beckman LS 6500 Scintillation System is a widely used and highly versatile detector that has been in service since the 1990s to measure the decay processes of various materials. Although it is large in size and requires a laboratory environment for its use, it can be programmed to automatically measure and print the results of over 640 samples with minimal user input [8].

In order to use the Beckman LS 6500 Scintillation System, a radioactive sample is measured out and mixed into a vial along with a "fluor," which is a solution that helps to create light based on the radioactive decay process. The fluor that was used during the research for this project was Ultima Gold, a product by PerkinElmer, Inc. Once the radioactive sample and the fluor are measured and poured into a vial, they are then placed into the Beckman Scintillation System as can be seen in Figure 1.

Figure 1. The Beckman LS 6500 Scintillation System used at Sagamore Adams Laboratories in Lafayette, Indiana.

The decay of the radioactive sample inside of the vial leads to the emission of ionizing radiation inside the vial, which, through the fluor, produces a number of photons that is related to the energy of the ionizing radiation itself. The ionization process produces photons that, over a nanosecond time scale, are emitted isotropically [8]. Once the photons are emitted from the vial, they are collected by specialized optics inside of the LS system, and directed into one of two photomultiplier tubes (PMTs). The PMTs are then activated by a photon burst, and convert the photons into electrical signals while simultaneously registering an individual nuclear decay event. Since it is likely that the PMTs are being hit by more than one photon simultaneously, the total number of photons produced can be found based on the proportional voltage pulse produced by the PMT. According to the operating manual, "The pulses from the PMTs are analyzed, converted to digital form, and stored in the appropriate channel of a multichannel analyzer, corresponding to the particle energy" [8]. It should be noted that the Beckman LS 6500 Scintillation System can discriminate between 32,768 energy levels based on its 32,768 channel multichannel analyzer. Based on the counting time of the sample, the rate (counts per minute, or cpm) of radioactive decay as well as the energy of the particles in the sample can be determined using the data from the multichannel analyzer. Specifically, the cpm count rate is calculated by dividing the total number of pulses in the multichannel analyzer by the total number of minutes that the LS system was counting that exact sample.

(1) Plutonium Experimentation and Analysis

Although the Beckman LS 6500 Scintillation system is quite accurate at discriminating between thousands of potential energy levels, in many cases it lacks a low enough detection threshold to detect radioactivity in diluted samples. To test the lower threshold of the Beckman LS 6500 Scintillation System, radioactive solutions of various dilutions were placed in the Beckman LS System for 60 minutes. They were then counted along with samples that contained no radioactivity whatsoever, for comparison. It should be noted that the radioactive solutions used by Sagamore Adams Laboratories, LLC, throughout the conduct of this research involved a "stock" solution of Pu-238 dissolved in acetone and a "stock" solution of Pu-239 dissolved in water.

In order to carry out this task, the mass of a bottle and a cap were measured individually and then filled with 15 mL of Ultima Gold fluor. Then, 0.5 mL of a Pu-238 solution (dissolved in acetone) was added to the bottle, which was sealed with the cap and its mass was again recorded. This process was then repeated with the same ingredients in order to have a second bottle of Pu-238 solution to verify the results of the first solution. Next, the process was repeated with a third and fourth bottle, this time containing a Pu-239 solution (dissolved in water) instead of the Pu-238 solution. Finally, two bottles were filled with 15 ml Ultima Gold and 0.5 mL water, and two more were filled with 15 mL Ultima Gold and 0.5 mL acetone, to provide a reference point for background measurements of water and acetone. All 8 bottles were then placed in the Beckman LS 6500 Scintillation System, and their radioactivity was measured over the course of 60 minutes each. The overall masses and individual contents of each bottle can be seen in Table 1, along with the cpm radioactivity measurement for each bottle as measured by the Beckman LS System.

Table 1. Masses and measured activity data of Pu-238, Pu-239, background acetone, and background water samples placed in Beckman LS 6500 Scintillation System for 60-minute individual measurements.

Sample ID	Contents	Mass of Bottle (g)	Mass of Cap (g)	Mass of Bottle, Cap, and 15mL Ultima Gold (g)	Mass of Bottle, Cap, 15mL Ultima Gold, and 0.5 mL Water/Acetone/Pu (g)	Mass of Solution (g)	Mass of Sample Added (g)	Measured Activity (cpm)
1	Ultima Gold and Acetone	13.0223	1.7310	29.3486	29.7345	14.9812	0.3859	64.72
3	Pu-238, Ultima Gold, Acetone	12.9707	1.6994	29.7266	30.1394	15.4693	0.4128	237.17
4	Pu-238, Ultima Gold, Acetone	12.9460	1.7525	29.7459	30.1646	15.4661	0.4187	245.48
5	Pu-239, Ultima Gold, Water	12.9335	1.7050	29.6817	30.1765	15.5380	0.4948	136.77
6	Pu-239, Ultima Gold, Water	13.0033	1.7364	29.7823	30.2840	15.5443	0.5017	137.37
7	Ultima Gold and Acetone	12.9026	1.7441	29.6810	30.0698	15.4231	0.3888	63.25
8	Ultima Gold and Water	12.9452	1.7754	29.7468	30.2331	15.5125	0.4863	65.48
9	Ultima Gold and Water	12.9585	1.7394	29.7252	30.2188	15.5209	0.4936	64.48

It should be noted that the sample ID skips the number 2 since there were issues with obtaining the mass of the number 2 sample bottle. A new sample bottle was then filled with acetone and Ultima Gold, and its mass was measured in a new sample bottle which can be seen as sample ID number 7. Further, as can be seen in Table 1, the Beckman was able to effectively discriminate between the activity levels of Pu-238 and Pu-239 solutions as compared to background levels. It should also be noted that this was with over 0.4 g of Pu-238 "stock" solution and nearly 0.5 g of Pu-239 "stock" solution placed in their respective bottles and then into the Beckman system.

The next task was to determine if the Beckman was able to discriminate between background levels and the radioactive isotopes when the isotopes were present in much more diluted solutions. In order to accomplish this, the "stock" Pu-238 and Pu-239 solutions were diluted in such a way that would produce an activity level of 0.1 Bq, or 1 disintegration every ten seconds. Carrying this dilution out, it was expected that an efficient detector (such as the CTMFD, which can be shown in chapter III) would register detection of a radioactive particle every ten seconds. At a minimum, an efficient detector should be able to discriminate between this new diluted solution and a control group solution of solely acetone or water. In order for a solution with an activity of 0.1 Bq to be created, the target specific activity of the new, diluted solutions needed to be calculated, which can be seen in Table 2.

Table 2. Calculations for volume of Pu-238 and Pu-239 stock solutions to be added to new, diluted solutions to be analyzed by Beckman LS 6500 Scintillation System.

Sample ID	Specific Activity (cpm/gram)	Average Specific Activity (cpm/gram)	Background Subtracted Specific Activity (cpm/gram)	Background Subtracted Specific Activity (Bq/gram)	Target Specific Activity (Bq/gram)	Volume of Solution (mL)	Mass of Solution (g)	Target Activity Added (Bq)	Target Mass Added (g)	Target Volume Added (mL)
1	167.712	165.20								
3	574.540									
4	586.291	580.42	415.22	6.92	0.0316	50.0000	39.5500	1.2498	0.1933	0.2444
5	276.415									
6	273.809	275.11	142.47	2.37	0.0316	50.0000	39.5500	1.2498	0.5263	0.5263
7	162.680	165.20								
8	134.649									
9	130.632	132.64								

The specific activity was calculated by taking the measured activity (cpm) and dividing it by the mass of the sample added (g). The average specific activity was then calculated by adding the specific activities of the two samples of each solution and dividing them by two to find the average. Next, the background specific activity was calculated by subtracting the acetone background specific activity from Pu-238, and the water background specific activity from Pu-239, since the stock solutions of Pu-238 and Pu-239 were dissolved in acetone and water, respectively. Next, the background specific activity was converted from cpm/gram to Bq/gram by dividing by 60, since 1Bq=1 disintegration per second or 60 disintegrations per minute.

In order to create the second solution with a target activity of about 0.1 Bq, the target specific activity first needed to be calculated. Since the density of the new solutions of Pu-238 and Pu-239 can be approximated by the density of acetone (since they are made up of only small amounts of the radioactive samples), and the sensitive bulb volume of the CTMFD is 4cc (to be detailed further in chapter III), the mass of the solution that could be kept in the sensitive portion of the CTMFD is calculated as follows:

$$0.791\frac{g}{cc} * 4cc = 3.164\,g\ of\ solution.$$

Since the target activity of the solution to be created is 0.1 Bq, or 1 disintegration every 10 seconds, then the target specific activity of the solution that could fit in the bulb is

$$\frac{0.1Bq}{3.164\,g} = 0.0316\frac{Bq}{g}.$$

The total volume of the new solution will be approximately 50 mL, which should allow enough to be used in both the Beckman LS System as well as for later use with the CTMFD to see if either can determine the difference between this new, diluted solution and background levels. Since the volume of the new, diluted solution will be 50 mL and the density is approximated to that of acetone, then the target mass of the new solution can be calculated as

$$0.791\frac{g}{cc} * 50\,cc = 39.55\,g\ of\ solution\,.$$

The target activity for these solutions should then be

$$0.0316\frac{Bq}{g} * 39.55\,g = 1.2498\,Bq\,.$$

To calculate the stock masses of both Pu-238 and Pu-239 to be added to the new solutions, the target activity calculated was divided by the background subtracted specific activity of both Pu-238 and Pu-239. The target masses of both solutions are:

Mass of Pu-238 solution: $$\frac{1.2498\,Bq}{6.92\frac{Bq}{g}} = 0.1806\,g\,,$$

and

Mass of Pu-239 solution: $$\frac{1.2498\,Bq}{2.37\frac{Bq}{g}} = 0.5273\,g\,.$$

Finally, since the density of the stock solution of Pu-238 can be approximated as acetone and Pu-239 can be approximated as water (as both solutions consist of mostly the acetone or water), the volume of each stock solution to be added to the new, diluted solutions can be calculated as:

Volume of Pu-238 solution: $$\frac{0.1806\,g}{0.791\frac{g}{cc}} = 0.228\,mL = 228\,\mu L\,,$$

and

Volume of Pu-239 solution: $$\frac{0.5273\,g}{1.00\frac{g}{cc}} = 0.527\,mL = 527\,\mu L\,.$$

From this information, the new, diluted solutions of both Pu-238 and Pu-239 were created, as can be seen in Table 3. Also note that 250 µL of Pu-238 was added instead of

228 µL, and 550 µL of Pu-239 was added instead of 527 µL, since the pipet used only allowed increments of 50 µL.

Table 3. Masses and activity calculations for new, diluted Pu solutions to be used in both CTMFD and Beckman LS 6500 Scintillation System.

Actinide	Mass of Nalgene (g)	Mass of Cap (g)	Mass of Nalgene, Cap, 50 mL Acetone (g)	Mass of Nalgene, Cap, 50 mL Acetone, Pu (g)	Mass of Pu Stock Solution Added (g)	Total Activity of Diluted Solution (Bq)	Mass of Solution (g)	Specific Activity of Diluted Solution (Bq/g)	Total Activity in Sensitive Volume (Bq)
Pu-238	14.4605	2.6030	56.6231	56.8116	0.1885	1.3044	39.7481	0.0328	0.1038
Pu-239	14.4811	2.5237	56.5720	57.1091	0.5371	1.2754	40.1043	0.0318	0.1006

As can be seen in Table 3, the total masses of the stock Pu solutions as well as the total activity of the diluted solutions are extremely close to the required values in Table 2. In the far right column of the Table 3, the expected time for emission/detection of a single radioactive particle is approximately 10 seconds (0.1 Bq). Now that the new, diluted solution had been created, it was necessary to put some of it into the Beckman LS System to determine if it could discriminate between this new, diluted solution and background levels of acetone. This was done by initially measuring the mass of an empty bottle and cap, and then adding 15 mL Ultima Gold and 1 mL of Pu-238, Pu-239, or acetone. Two bottles were created of each, for a total of 6 bottles, to ensure that each sample had a consistent reading. The data for the new solutions placed in the Beckman system can be seen in Table 4.

Table 4. Masses and measured activity data of diluted Pu-238, diluted Pu-239, and background acetone samples placed in Beckman LS 6500 Scintillation System for 60-minute individual measurements.

Sample ID	Contents	Mass of Bottle (g)	Mass of Cap (g)	Mass of Bottle, Cap, and 15mL Ultima Gold (g)	Mass of Bottle, Cap, 15mL Ultima Gold, and 1 mL Acetone or Pu (g)	Mass of Solution (g)	Mass of Sample Added (g)	Measured Activity (cpm)	1 σ Error (cpm)
1	Acetone and Ultima Gold	12.9365	1.7386	29.6842	30.4575	15.7824	0.7733	62.80	2.05
2	Acetone and Ultima Gold	12.9327	1.7149	29.6649	30.4378	15.7902	0.7729	64.03	2.07
3	Diluted Pu-238, Ultima Gold	12.9454	1.7629	29.7239	30.5014	15.7931	0.7775	62.70	2.04
4	Diluted Pu-238, Ultima Gold	12.9366	1.7564	29.7070	30.4857	15.7927	0.7787	61.47	2.02
5	Diluted Pu-239, Ultima Gold	12.9906	1.7147	29.7163	30.4990	15.7937	0.7827	63.28	2.06
6	Diluted Pu-239, Ultima Gold	12.9796	1.7224	29.7181	30.4960	15.7940	0.7779	61.97	2.03

As can be seen in Table 4, the Beckman LS 6500 Scintillation System was unable to discriminate between solutions containing diluted Pu-238, diluted Pu-239, and acetone alone. In Table 5, the error calculations show that even with reasonable error factored into the Beckman LS measurements, it still cannot discriminate between the various radioactive solutions and background levels.

The percent error calculations are determined by the Beckman machine (using standard Poisson counting statistics and accounting for any electrical noise) and are shown on the printout that is collected from the printer (see Figure 2). The 1σ error in cpm was then calculated by multiplying the percent error by the measured activity in the same row of Table 4. The specific activity in cpm/gram was calculated by dividing the measured activity by the mass of the sample added (both from Table 4). The 1σ error in cpm/gram was calculated by dividing the 1σ error in cpm by the mass of the sample added in grams. The next column shows the average specific activity of the two samples of each solution, which is used to minimize the discrepancies in any one bottle of solution. The average for the 1σ error is calculated differently than a traditional average, and is calculated using the formula

$$\sigma = \frac{\sqrt{\left(value1^2 + value2^2\right)}}{2}$$

instead of

$$\sigma = \frac{\left(value1 + value2\right)}{2},$$

as discussed in the Knoll reference [5]. The background subtracted specific activity is calculated by taking the average specific activity of the solutions for Pu-238 and Pu-239, and subtracting the value of the average specific activity for the background solutions of acetone. The 1σ error average of the Pu-238 and acetone and Pu-239 and acetone are calculated by using the Poisson formula again,

$$\sigma = \frac{\sqrt{\left(value1^2 + value2^2\right)}}{2}.$$

Table 5. Error calculations of diluted Pu-238, diluted Pu-239, and background acetone samples placed in Beckman LS 6500 Scintillation System for 60-minute individual measurements.

Sample ID	Specific Activity (cpm/gram)	1 σ Error (cpm/gram)	Average Specific Activity (cpm/gram)	1 σ Error (cpm/gram)	Background Subtracted Specific Activity (cpm/gram)	1 σ Error (cpm/gram)	Background Subtracted Specific Activity (Bq/gram)	1 σ Error (Bq/gram)
1	81.210	2.647						
2	82.844	2.676	82.027	1.882				
3	80.643	2.629						
4	78.939	2.597	79.791	1.848	-2.24	2.64	-0.04	0.04
5	80.848	2.628						
6	79.663	2.613	80.256	1.853	-1.77	2.64	-0.03	0.04

As can be seen in Table 5, the background subtracted specific activity of the diluted Pu-238 solution that was placed in the Beckman had a value of -2.24. Given that the 1σ error was larger than this value (2.64), this shows that the Beckman LS 6500 Scintillation System is unable to discriminate between the diluted Pu-238 solution and background solutions. Similarly, for the diluted Pu-239 solution, the value of the background subtracted specific activity in cpm/gram (-1.77) was less than the 1σ error (2.64). This only further demonstrates the fact that the Beckman Scintillation System is unable to discriminate between highly diluted radioactive solutions and background levels. The last two columns in Table 5 also show that the Beckman is unable to discriminate between diluted radioactive solutions and background levels, but use units of Bq/gram as opposed to cpm/gram.

PAGE: 1

ID:PU DILUTE ACE 22 SEP 2015 15:48
USER: 8 COMMENT:PU238 PU239
PRESET TIME : 60.00
DATA CALC : CPM H# :YES SAMPLE REPEATS: 1 PRINTER :EDIT
COUNT BLANK : NO IC# : NO REPLICATES : 1 RS232 : OFF
TWO PHASE : NO AQC : NO CYCLE REPEATS : 1
SCINTILLATOR: LIQUID LUMEX: NO LOW SAMPLE REJ: 0
LOW LEVEL : NO HALF LIFE CORRECTION DATE: none

WIDE OPEN WINDOW %ERROR: 0.00 FACTOR: 1.000000 BKG. SUB: 0

	SAM NO	POS	TIME MIN	H#	WIDE CPM	WIDE %ERROR	LUMEX %	ELAPSED TIME
Acc	1	**-1	60.00	86.1	62.80	3.26	0.72	61.02
Acc	2	**-2	60.00	87.1	64.03	3.23	0.62	122.14
Acc 238	3	**-3	60.00	86.9	62.70	3.26	0.72	183.27
Acc 238	4	**-4	60.00	87.7	61.47	3.29	0.70	244.40
Acc 239	5	**-5	60.00	87.6	63.28	3.25	0.53	305.50
Acc 239	6	**-6	60.00	86.3	61.97	3.28	0.51	366.59

Diluted vs Background (22 Sept)

Figure 2. Printout from Beckman LS 6500 Scintillation System containing data used in Tables 4 and 5.

(2) Uranyl Nitrate Experimentation and Analysis

Although the previous section demonstrates that the Beckman LS 6500 Scintillation System is unable to discriminate between diluted plutonium solutions and background levels, it is necessary to test and measure diluted solutions of other radioactive isotopes as well to ensure that plutonium is not an outlier. This was done in a manner similar to that of the Pu-238 and Pu-239 solutions as described previously. Unlike the Pu-238 and Pu-239 solutions, however, the Uranyl Nitrate samples come in a solid form, and therefore a solution needed to be created with a measured amount of the UN crystals and 50 mL of acetone. The mass of a small bottle and cap was measured and then filled with 50 mL of acetone, and its mass was measured again. Next, a small UN nugget was added and allowed to dissolve. The total mass of the bottle, cap, and new solution were then measured again for a final time. The mass of the solution created can be seen in Table 6.

Table 6. Masses of bottle, cap, 50 mL of acetone, and UN nugget used to create UN stock solution for Beckman LS 6500 Scintillation System analysis.

Mass of Bottle and Cap (g)	Mass of Bottle, Cap, and 50mL Acetone (g)	Mass of Bottle, Cap, 50mL Acetone, and UN (g)	Mass of UN added (g)
20.4430	58.9854	58.9989	0.0135

Now that a Uranyl Nitrate solution had been created, it was then necessary to ensure the Beckman could discriminate between this highly concentrated solution and background levels of acetone. In order to do this, 0.5 mL of the concentrated solution of Uranyl Nitrate was placed into each of two separate bottles whose mass had already been measured. 15 mL of Ultima Gold was also placed into each bottle, which was then moved into the Beckman LS Scintillation System for 60-minute readings (along with two bottles of only acetone to measure the background). The results of the mass measurements and measured activity readings from the Beckman LS Scintillation System can be seen in Table 7.

Table 7. Masses and measured activity data of Uranyl Nitrate and background acetone samples placed in Beckman LS 6500 Scintillation System for 60-minute individual measurements.

Sample ID	Contents	Mass of Bottle (g)	Mass of Cap (g)	Mass of Bottle, Cap, and 15mL Ultima Gold (g)	Mass of Bottle, Cap, 15mL Ultima Gold, and 0.5 mL Acetone/UN (g)	Mass of Solution (g)	Mass of Sample Added (g)	Measured Activity (cpm)
1	Acetone and Ultima Gold	12.9814	1.4271	29.7014	30.0901	15.6816	0.3887	62.68
2	Acetone and Ultima Gold	12.8372	1.4908	29.5644	29.9598	15.6318	0.3954	61.32
3	UN, Ultima Gold, Acetone	12.9220	1.7316	29.6616	30.0515	15.3979	0.3899	410.68
4	UN, Ultima Gold, Acetone	12.9348	1.7678	29.7183	30.1064	15.4038	0.3881	408.30

As can be seen in the last column of Table 7, the Beckman Scintillation System was able to easily discriminate between the activity of the "stock" Uranyl Nitrate solution and the activity of a background acetone solution. Since the Beckman was able to discriminate between the activity of Pu-238 and Pu-239 and background acetone, it was entirely expected that the same result would occur for this Uranyl Nitrate solution. The next step was to dilute the UN solution to an activity that is roughly 2% of that of the stock solution, and determine whether or not it could be detected by the Beckman system. Table 8 is a continuation of Table 7, but the last six columns provide the means for calculating the total volume of stock solution to be added to create the new, diluted solution.

Table 8. Calculations for volume of UN stock solution to be added to new, diluted solution to be analyzed by Beckman LS 6500 Scintillation System.

Specific Activity (cpm/gram)	Average Specific Activity (cpm/gram)	Background Subtracted Specific Activity (cpm/gram)	Background Subtracted Specific Activity (Bq/gram)	Target Specific Activity (Bq/gram)	Volume of Solution (mL)	Mass of Solution (g)	Target Activity Added (Bq)	Target Mass Added (g)	Target Volume Added (mL)
161.255									
155.083	158.17								
1053.296									
1052.048	1052.67	894.50	14.91	0.0316	50.0000	39.5500	1.2498	0.0838	0.1060

The first four columns of Table 8 are merely calculations for the background subtracted specific activity of the stock UN solution that was analyzed by the Beckman system. The manner in which the values for these columns were calculated are exactly the same as was done for the stock Pu-238 and Pu-239 solutions that were calculated in Table 2. The target specific activity of the new, diluted solution was calculated in the same way as was used for the diluted Pu-238 and Pu-239 solutions, where the density of acetone is assumed and multiplied by the volume of the solution to be created:

$$0.791\frac{g}{cc} * 50\,cc = 39.55\,g\ of\ solution\,.$$

Then, this mass calculated above is multiplied by the target specific activity of 0.0316 Bq/g, which is based on the volume of the bulb of the CTMFD (to be discussed further in chapter III). The target activity added is then

$$0.0316\frac{Bq}{g} * 39.55\,g = 1.2498\,Bq\,.$$

The target mass added is then found by dividing the target activity added by the background subtracted specific activity that was found from the stock solution, and is calculated as

$$\frac{1.2498\,Bq}{14.91\,Bq/g} = 0.0838\,g\,.$$

The volume of the stock solution to be added to create this new solution, then, can be seen in the far right of Table 8 and is calculated by dividing the mass above by the density of acetone:

$$\frac{0.0838\,g}{0.791\,g/cc} = 0.106\,mL\,.$$

In order to create this new solution, the mass of a small bottle and cap was measured, filled with 50 mL of acetone, and then its mass was measured again. Next, 0.106 mL of the stock UN solution was placed into the bottle and the mass of the bottle and cap was

measured again for a third and final time. The measurements for this new bottle of the diluted solution can be seen in Table 9.

Table 9. Masses and activity calculations for new, diluted UN solution to be used in both CTMFD and Beckman LS 6500 Scintillation System.

Actinide	Mass of Nalgene and Cap (g)	Mass of Nalgene, Cap, 50 mL Acetone (g)	Mass of Nalgene, Cap, 50mL Acetone, 0.106 mL UN solution (g)	Mass of UN Stock Solution Added (g)	Total Activity of Diluted Solution (Bq)	Mass of Solution (g)	Specific Activity of Diluted Solution (Bq/g)
UN	20.3539	57.9326	58.0164	0.0838	1.2500	37.6625	0.0332

Table 10. Masses and measured activity data of diluted UN and background acetone samples placed in Beckman LS 6500 Scintillation System for 60-minute individual measurements.

Sample ID	Contents	Mass of Bottle (g)	Mass of Cap (g)	Mass of Bottle, Cap, and 15mL Ultima Gold (g)	Mass of Bottle, Cap, 15mL Ultima Gold, and 1 mL Acetone or UN (g)	Mass of Solution (g)	Mass of Sample Added (g)	Measured Activity (cpm)	% Error
1	Acetone and Ultima Gold	12.9365	1.7386	29.6842	30.4575	15.7824	0.7733	62.80	3.26
2	Acetone and Ultima Gold	12.9327	1.7149	29.6649	30.4378	15.7902	0.7729	64.03	3.23
3	Diluted UN, Ultima Gold	12.9602	1.7250	29.7112	30.4850	15.7998	0.7738	64.78	3.21
4	Diluted UN, Ultima Gold	12.9121	1.7801	29.6936	30.4803	15.7881	0.7867	62.08	3.28

As can be seen in Table 9, the specific activity of the diluted solution was found to be extremely close to the target specific activity of 0.0316 Bq/g. Now, having created this new diluted solution, it was time to place 1 mL of the new solution into each of two bottles, along with 15 mL of Ultima Gold. Two other bottles were also filled with 15 mL of Ultima Gold and acetone, acting as a background reference point. The masses of all four bottles and their contents were measured, and then placed into the Beckman LS 6500 Scintillation System for 60-minute individual measurements to measure the activity of each sample. The results of these measurements can be seen in Table 10.

Clearly, the Beckman LS 6500 Scintillation System was not able to discriminate between this new, diluted UN solution and background solutions of acetone alone. Table 11 shows that even with error calculations (calculated in the same manner as those of Pu-238 and Pu-239 in Table 5), the Beckman system still cannot discriminate between the two solutions.

Table 11. Error calculations of diluted UN and background acetone samples placed in Beckman LS 6500 Scintillation System for 60-minute individual measurements.

Sample ID	1 σ Error (cpm)	Specific Activity (cpm/gram)	1 σ Error (cpm/gram)	Average Specific Activity (cpm/gram)	1 σ Error (cpm/gram)	Background Subtracted Specific Activity (cpm/gram)	1 σ Error (cpm/gram)	Background Subtracted Specific Activity (Bq/gram)	1 σ Error (Bq/gram)
1	2.05	81.21	2.65						
2	2.07	82.84	2.68	82.03	1.88				
3	2.08	83.72	2.69						
4	2.04	78.91	2.59	81.31	1.87	-0.71	2.65	-0.01	0.04

(3) Conclusions

Although the Beckman LS 6500 Scintillation System is quite effective at discriminating between thousands of potential energy levels, in many cases it lacks a low enough detection threshold to detect radioactivity in diluted samples. As can be seen in Table 1, the Beckman LS System was clearly able to discriminate between highly concentrated samples of Pu-238, Pu-239, and background samples of acetone and water. Table 7 also shows that the Beckman LS System could discriminate between the highly concentrated solution of UN and a solution of acetone alone. However, once the solutions were diluted to levels that were about 1–2% of the concentration of the original solution, the Beckman could not discriminate between Pu-238, Pu-239, UN, and/or background samples of acetone. This goes to show that while the Beckman is very effective at detection and discrimination of stronger samples, it does not have a low enough threshold to detect radioactive solutions that are highly diluted. It is also extremely large, immobile, and contains highly sensitive equipment worth thousands of dollars. The Beckman LS 6500 is not likely to be used by DTRA or the military services in an austere environment or in any environment outside that of a secure laboratory.

b. NE-213 Liquid Scintillator

While often not as efficient as organic scintillator crystals, liquid scintillators are generally cheaper and easier to manufacture. Unlike more traditional organic scintillators, the NE-213 uses a toxic solvent such as xylene as the scintillation material, which then produces amounts of light that are proportional to the energy deposited by neutrons or gamma rays [9]. Different particles interacting with the scintillator will produce different "pulse shapes" on a plot of light intensity versus time, or a plot of number of counts versus pulse shape discrimination (PSD). For instance, a neutron interacting with the liquid scintillator will produce a dissimilar light intensity and time dependence than a gamma particle interacting with the scintillator. Previous work on NE-213 scintillators (Figure 3) shows how the pulse shape is different for neutrons and gamma rays:

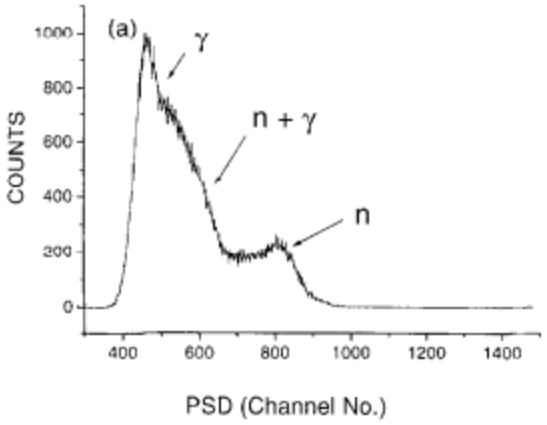

Figure 3. Graph of single spectrum of pulse-shape discrimination for NE-213 liquid scintillator as measured by Lee and Lee. Adapted from [10].

The sensitivity of the detector can be adjusted based on the initial readings, and gamma rays can be nearly entirely discriminated out, leaving only readings for fast neutrons. It should also be noted that Lee and Lee also determined that the Compton edge for ^{60}Co is approximately equivalent in light output to 2.7 MeV neutrons. As will be discussed in the next section, lowering the discriminator level to the Compton edge of ^{60}Co will allow for rejection of roughly 99.9% of gamma rays [10].

It should also be noted that the goal of this study is to evaluate and compare various detectors for their practical use in military and specifically battlefield applications. The NE-213 has an extensive and cumbersome equipment setup, and also requires an outside radioactive source for calibration. The equipment chain that was used for the NE-213 liquid scintillator throughout the course of this research can be seen in Figure 4 and Table 12.

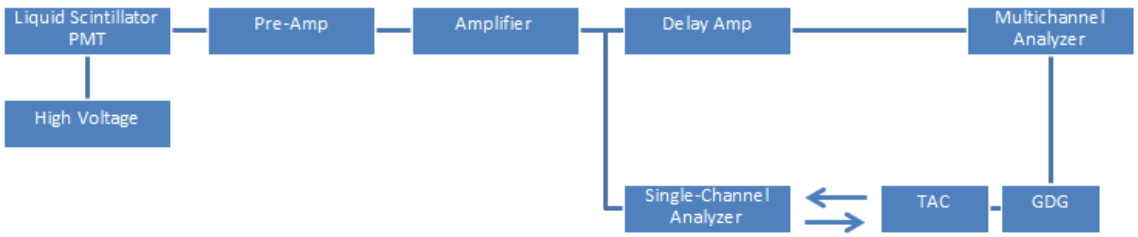

Figure 4. Visual layout of equipment string used for NE-213 liquid scintillator during the conduct of this research.

Table 12. Equipment listing for experiments carried out with NE-213 liquid scintillator.

Equipment	Manufacturer/Model
NE-213 LS Detector	ORTEC 265
Pre-Amplifier	ORTEC 113
Amplifier	ORTEC 460
Single Channel Analyzer	ORTEC 552
High Voltage	Stanford PS350
Time to Amplitude Converter (TAC)	Canberra 2145
Gate Delay Generator (GDG)	ORTEC 416A
Delay Amplifier (DA)	SpecTech 427A
Multichannel Analyzer	Agilent UCS-20

Although it can be seen that the equipment string is complex and the calibration time can be tedious and difficult, it is still appropriate to evaluate the overall performance of the NE-213 detector itself with regard to neutron detection efficiency.

(1) Experimentation and Analysis

Once the equipment was set up and powered on in the laboratory environment, it was time to calibrate the detector with two separate gamma sources, cobalt-60 and cesium-137. To do this, the NE-213 detector was first assembled using the equipment described in Table 12, and then a Co-60 source was placed in close proximity to the LS portion of the detector. Next, UCS30 software was used to determine the number of counts that were received in each energy-related channel over the course of 300 seconds. The results of the Co-60 readings can be seen in Figures 5 and 6, with the y-axis in both logarithmic and linear scales.

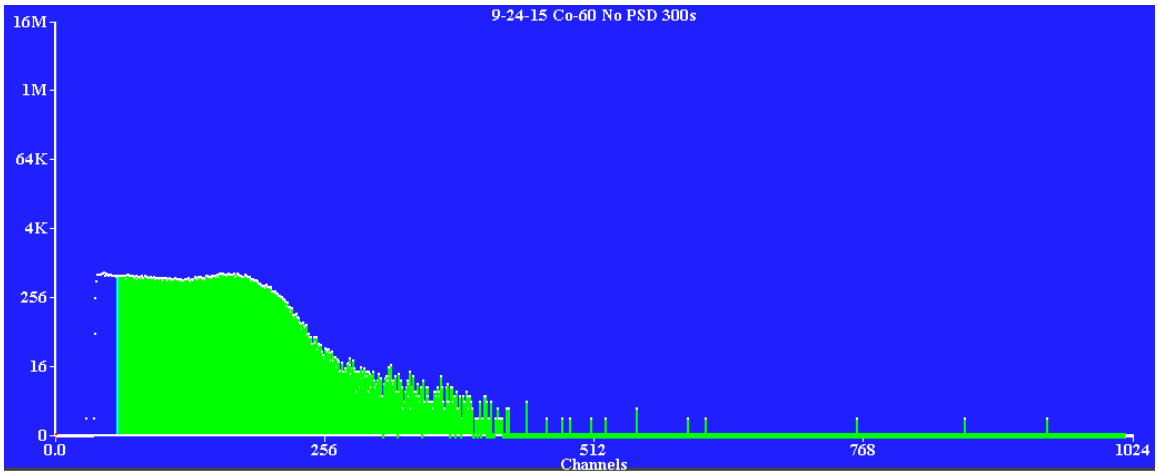

Figure 5. UCS30 software output of number of counts vs. channel number for a Co-60 source (y-axis is logarithmic scale).

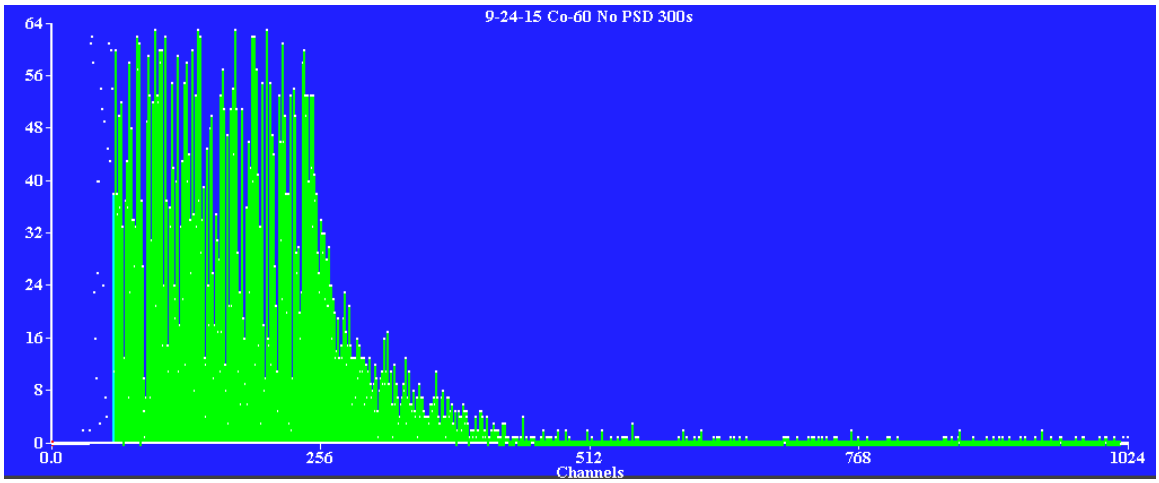

Figure 6. UCS30 software output of number of counts vs. channel number for a Co-60 source (y-axis is linear scale).

Using the data in Figure 6, it was then necessary to determine which channel number is related to the maximum energy of Compton-recoiled electrons associated with a Cobalt-60 source. It would then be possible to calibrate the x-axis of the software output with a specific energy reading. According to Lee and Lee, "the maximum energy of Compton-recoiled electrons corresponds to the position 80% down the height of the Compton edge" [10]. Based on Figures 5 and 6 (and more specifically using the UCS30 software itself), it can be determined that the peak of the output occurs at channel 164. The endpoint is slightly more arbitrary, as pulse pile-up makes it difficult to determine a

sharp endpoint. Pulse pile-up occurs when two readings are registered simultaneously, and appear as an event much higher than what a single gamma could create. However, using the linear y-axis scale in Figure 6, it can be seen that the sharpest drop (and most likely to be associated with the beginning of pulse pile-up) occurs at channel 256. Now that the peak and endpoint of the Compton edge have been determined, simple mathematics can be used to find the point 80% down the edge, which is related to the maximum energy of Compton-recoiled electrons. Since the detector is being calibrated for fast neutrons, the neutron energy (proton recoil energy) can be found using Figure 7 to correlate the electron energy (found as described previously) with the proton recoil energy.

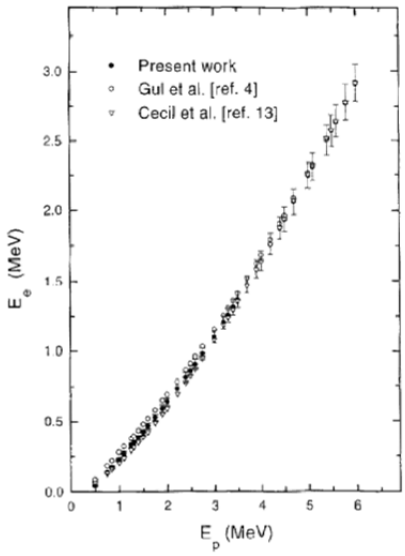

Figure 7. Plot of the relationship between electron recoil energy and proton recoil energy for a NE-213 liquid scintillator as compared by Lee and Lee. Adapted from [10].

This process was repeated with cesium-137, and the associated peaks and endpoints were evaluated along with determining the related electron, proton, and neutron energies. Tables 13 and 14 show the channel numbers as well as the associated particle energies for both the cobalt-60 and cesium-137 sources.

Table 13. Channel number/energy calibration for NE-213 using cobalt-60 source.

Position	Channel No.
Peak	164
Endpoint	256
Midpoint	210
80% point*	238

Note that midpoint position here corresponds to 1.33 MeV electron energy resulting from gamma ray interaction, and the 80% point corresponds to 3.5 MeV proton energy resulting from neutron interaction.

Table 14. Channel number/energy calibration for NE-213 using cesium-137 source.

Position	Channel No.
Peak	72
Endpoint	118
Midpoint	95
80% point*	109

Note that midpoint position here corresponds to 0.661 MeV electron energy resulting from gamma ray interaction, and the 80% point corresponds to 2 MeV proton energy resulting from neutron interaction.

Using the channel numbers associated with the electron and proton energies as seen in Tables 14 and 15, the UCS30 software could then be used to calibrate the x-axis of the plots to sort the incoming particles by associated neutron energies instead of by channel number. The second and final stage of calibration involved adjusting the sensitivity of the NE-213 to discriminate against any incoming gamma radiation using pulse shape discrimination (PSD). To do this, a Cobalt-60 source was placed 50 cm from the NE-213 detector, and initial readings were taken without pulse shape discrimination rejecting any readings (T value of 0.10). The T value was then adjusted to discriminate against various parts of the pulse shape. Two readings were then taken at a time of 60 seconds apiece: one with the Co-60 source present, and the second without any radioactive source present to determine the background readings that were measured at each T value. By repeating this reading over a range of T values (as can be seen in Table

15), eventually the T values associated with 99.0% and 99.9% rejection were able to be determined.

Table 15. Calibration of NE-213 detector to 99.0% and 99.9% rejection of gamma rays using Co-60 over a range of T values.

Source	Time (s)	T Value	Background Counts	Gross Counts	Background Subtracted Gross Counts	PSD (% Rejection)
Co-60	60	0.10	603	18925	18322	N/A
Co-60	60	2.00	0	4	4	99.98
Co-60	60	1.50	67	922	855	95.33
Co-60	60	1.70	4	46	42	99.77
Co-60	60	1.65	0	70	70	99.62
Co-60	60	1.60	14	130	116	99.37
Co-60	60	1.55	20	334	314	98.29
Co-60	60	1.58	12	203	191	98.96
Co-60	120	1.8	2	38	36	99.90

Note that the last two rows of the table correspond to roughly 99.0% and 99.9% rejection of gamma rays due to pulse shape discrimination.

Now that the UCS30 software as well as the NE-213 detector had been calibrated to discriminate out up to 99.0 percent and 99.9 percent of incoming gamma rays, the detector itself could be used to detect neutrons emitted from a point source. The overall goal was to determine the efficiency of the NE-213 system at detecting neutrons from a Cf-252 source as well as from a Pu-Be source, at distances of 50 cm and 100 cm. This was to be done with the detector adjusted to discriminate out 0%, 99.0%, and 99.9% of gamma rays, to compare the efficiencies of fast neutron detection.

Figure 8. Photo of experimental setup of NE-213 liquid scintillator using a Cf-252 neutron source from a distance of 50 cm.

The experimentation phase itself began by placing a Cf-252 source 50 cm from the detector (see Figure 8). The software was adjusted to initially reject 0% of the gamma rays, and measure the data recorded over the course of two minutes. The gross counts were measured to be 2,872, and the background counts were previously measured to be 1,206. This left the background counts at 1,666 over two minutes, or 13.833 counts per second. Based on the averaging of gamma data from previous research, the neutron to gamma emission ratio for Cf-252 is found to be roughly 3.8:8 [5], [11]. Therefore, the fluence of neutrons passing through an area of 1 cm^2 at a distance of 50 cm can be calculated using the formula

$$\Phi = \frac{N}{4\pi d^2} \quad ,$$

where Φ is the fluence in neutrons/cm^2/sec, N is the number of neutrons emitted by the source, and d is the distance from the source [5]. In order to calculate the N value, the last known activity measurement of the source was used to calculate the current activity of the source using the formula

$$\alpha = \alpha_0 e^{-\lambda t},$$

where α is the current activity, α_0 is the previous activity, λ is the decay constant, and t is the time since the previous activity measurement. Since the last activity measurement (18.5 MBq) was on 1 June 2002, the time value between that date and 20 September 2015 is 419.904×10^6 seconds. The decay constant λ, using a half-life of 2.645 years, is found to be 8.30985×10^{-9} seconds^{-1}.

Therefore, using the formula above and plugging in the above values, the current activity is

$$\alpha = (18.5\,MBq)\, e^{-(8.30985 x 10^{-9}\, s^{-1})(419.904 x 10^6\, s)} = 564.639\,kBq.$$

Based on the table of nuclides from the Korea Atomic Energy Research Institute (KAERI), the spontaneous fission (SF) branch ratio is 3.09%, which can be multiplied by the current activity above to find the number of fissions per second [12]:

$$(564639\,Bq)(0.0309) = 17447.3\ \textit{fissions per second}.$$

Now, the only remaining step is to multiply this value for fissions per second by the neutrons and gammas being produced per fission. For the case of 0% PSD, this would be

$$(17447.3\ \textit{fissions per second})(3+8).$$

For cases where 99.0% and 99.9% of the gammas were rejected, the value of 8 in the above equation was multiplied by 0.01 and 0.001, respectively. Now that the N value has been obtained, the only remaining variable in the fluence equation is d, for the distance of the detector from the source. This will be either 50 cm or 100 cm, as both distances were used for both a Pu-Be source and a Cf-252 source. This fluence value is then multiplied by the cross sectional area of the detector, which is 25 cm^2, to obtain the total number of neutrons per second through the sensitive volume of the NE-213 scintillator. Using the value for background subtracted gross counts per second as described above, and dividing that value by the total number of neutrons per second through the sensitive volume of the detector, the intrinsic detection efficiency can be obtained. These calculations were done for both a Cf-252 source as well as a Pu-Be source, at distances of

50 cm and 100 cm, at 0%, 99.0%, and 99.9% gamma rejection. The only differences in the calculations for the Pu-Be source is that the neutron to gamma emission ratio is 1:1, and the activity is 2.2×10^6 fissions per second. The results for the experimental data as well as the calculated values for intrinsic detection efficiency for both sources at the distances and PSD settings described previously can be seen in Table 16.

Table 16. Experimental data and intrinsic neutron detection efficiency results for NE-213 liquid scintillator using Cf-252 and Pu-Be sources.

Source	PSD (% Rejection)	Distance (cm)	Time (s)	Gross Counts	Background Counts	Background Subtracted Gross Counts	Background Subtracted Gross Counts per Second	Neutron: Gamma Emission Ratio	Fluence (neutrons/cm^2/sec)	Total Neutrons Through Sensitive Volume (neutrons/s)	Intrinsic Detection Efficiency
Cf-252	0.0%	50	120	2,872	1,206	1,666	13.883	3.8:8	6.553305	163.832618	8.47%
Cf-252	99.0%	50	120	472	24	448	3.733		2.154815	53.870386	6.93%
Cf-252	99.9%	50	120	305	4	301	2.508		2.114829	52.870730	4.74%
Cf-252	0.0%	100	120	1,691	1,206	485	4.042		1.638326	40.958155	9.87%
Cf-252	99.0%	100	120	137	24	113	0.942		0.538704	13.467597	6.99%
Cf-252	99.9%	100	120	78	4	74	0.617		0.528707	13.217682	4.67%
Pu-Be	0.0%	50	120	57,258	1,206	56,052	467.100	1:1	140.056350	3501.408748	13.34%
Pu-Be	99.0%	50	120	33,923	24	33,899	282.492		70.728457	1768.211418	15.98%
Pu-Be	99.9%	50	120	26,812	4	26,808	223.400		70.098203	1752.455078	12.75%
Pu-Be	0.0%	100	120	16,575	1,206	15,369	128.075		35.014087	875.352187	14.63%
Pu-Be	99.0%	100	120	9,027	24	9,003	75.025		17.682114	442.052854	16.97%
Pu-Be	99.9%	100	120	7,209	4	7,205	60.042		17.524551	438.113770	13.70%

As can be seen by the data in Table 16, the NE-213 liquid scintillator was capable of detecting up to 8.47% of neutrons from a Cf-252 source at a distance of 50 cm, and up to 9.87% of incident neutrons from a Cf-252 source at a distance of 100 cm. For the Pu-Be source, the NE-213 liquid scintillator detected 15.98% of incident neutrons from a distance of 50 cm, and up to 16.97% of incident neutrons from a distance of 100 cm. It should be noted that the highest intrinsic detection efficiencies for the Cf-252 source were found when 0% of gamma rays were rejected by the detector. Notably, this was different for the Pu-Be source, which found that the highest detection efficiency was achieved when 99.0% of gamma rays were rejected for both distances of 50 cm and 100 cm. This is a bit different than what was expected, considering that none of the highest neutron detection efficiencies were achieved when the highest amount of gamma rays were rejected (99.9%), and the highest detection efficiencies were not achieved at the same percentage of gamma rejection for both Cf-252 and Pu-Be sources.

(2) Conclusions

First and foremost, it should be noted that the NE-213 liquid scintillator is much more suitable for a laboratory environment than a military environment. Utilizing an equipment string of more than nine pieces, it is cumbersome to set up and calibrate, and is not mobile by any means. Once set up, a gamma source is needed to calibrate the detector for discrimination against gamma rays, which is a tedious and somewhat subjective process. Once calibration is complete, the detector must take several different readings at different levels of gamma discrimination to determine the highest possible detection rate. Further, the highest amount of discrimination against gamma rays does not necessarily coincide with the highest intrinsic detection efficiency of fast neutrons, which is counterintuitive. The highest detection efficiency will be achieved at different gamma discrimination levels for different neutron sources. Nevertheless, the NE-213 did prove to have relatively high neutron detection efficiencies at various distances from both neutron sources, at all levels of gamma discrimination. The lowest intrinsic detection efficiency was found to be 4.67%, which is still higher than the detection efficiency of any other detector used during the course of this study.

2. Boron Trifluoride Neutron Detector

Unlike the scintillation principle used by the Beckman LS 6500 Scintillation System and NE-213 liquid scintillator, the boron trifluoride detector uses an aluminum tube filled with BF_3 gas to interact with incoming neutrons. The boron gas is often enriched with boron-10 atoms, which results in an efficiency up to five times greater than if only naturally occurring boron is used [5]. When a boron-10 atom absorbs an incoming neutron, a recoil lithium-7 nucleus and an alpha particle are produced, and travel in opposite directions towards the detector wall. The detector will measure a pulse that is dependent upon whether or not the lithium-7 nucleus was left in the ground state or in the excited state. If left in the ground state, the lithium-7 nucleus and the alpha particle are left with more energy to create ion pairs, and thus have a higher kinetic energy. This occurs roughly 6% of the time, and results in a total kinetic energy of about 2.792 MeV between the two particles. The other 94% of the time, the lithium nucleus is left in the excited state, and the resulting total kinetic energy of the two particles is only about 2.310 MeV [13]. Figure 9 shows the expected pulse shape of a BF_3 detector from a neutron source, including annotation for the discrimination of gamma rays and noise.

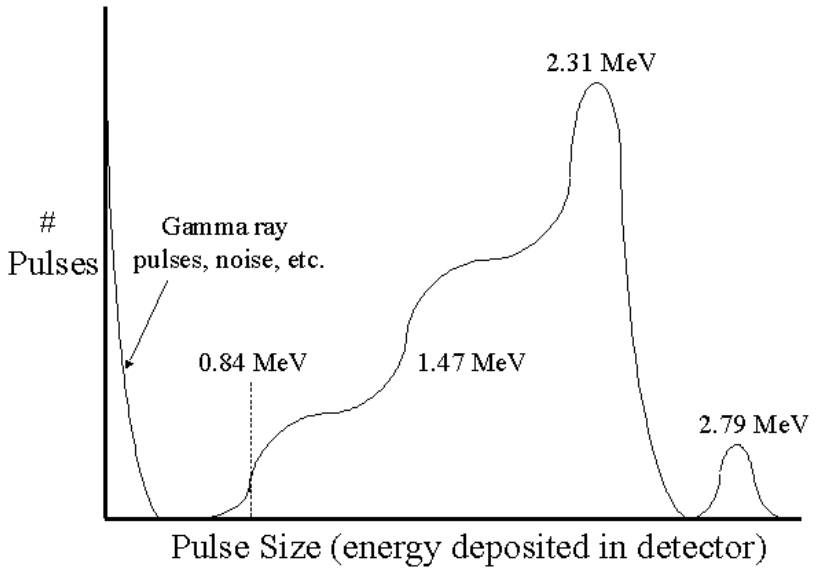

Figure 9. Expected pulse shape discrimination for a BF_3 detector interacting with a neutron source. Adapted from [13].

It can be seen from Figure 9 that the gamma rays can be discriminated out by simply setting the detector threshold above this pulse size. It is also important to note that BF_3 detectors are not effective at detecting fast neutrons unless the metal detector tube is surrounded by a moderator. For the boron trifluoride neutron detector used in this experiment, the detector tube was surrounded by a high-density polyethylene sphere, which slowed down the fast neutrons and converted them to thermal neutrons. Figure 10 shows a photo of the aluminum tube of the detector next to the polyethylene sphere used to convert the fast neutrons.

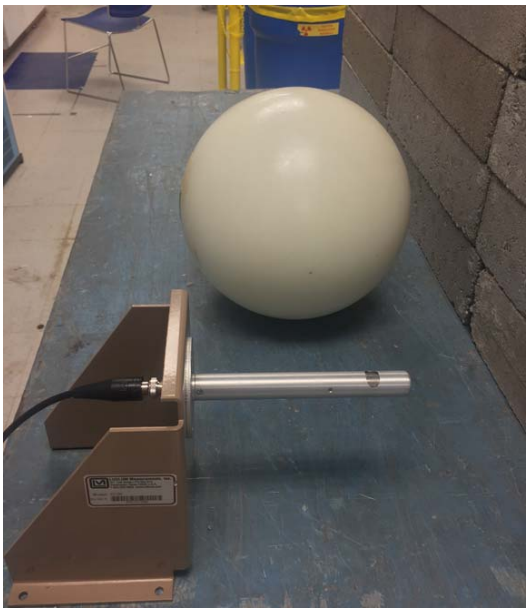

Figure 10. Photo of polyethylene sphere and aluminum tube filled with BF_3 which were used in this study to acquire experimental data.

It should again be noted that the goal of this study is to evaluate and compare various detectors for their practical use in military and specifically battlefield applications. Like the NE-213 liquid scintillator, the boron trifluoride detector has an extensive and cumbersome equipment setup, and also requires an outside radioactive source to calibrate. The equipment chain that was used for the boron trifluoride detector throughout the course of this research can be seen in Figure 11 and Table 17.

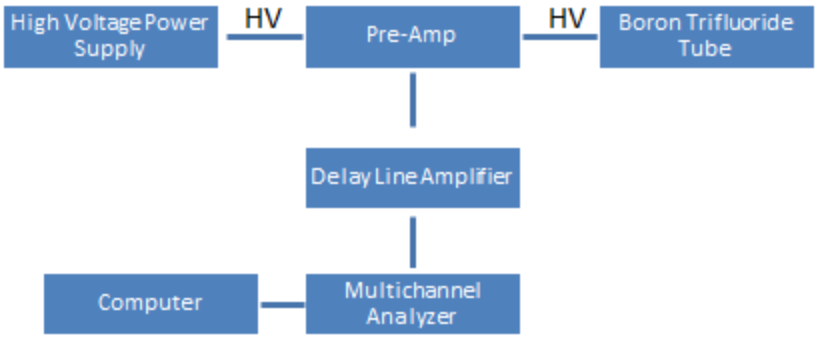

Figure 11. Visual layout of equipment string used for BF_3 detector during the conduct of this research.

Table 17. Equipment listing for experiments carried out with BF_3 detector.

Equipment	Manufacturer/Model
BF_3 Detector	Ludlum Model 42–30
High Voltage Power Supply	Stanford PS325
Pre-Amplifier	ORTEC 142
Delay Amplifier (DA)	ORTEC 460
Multichannel Analyzer	UCS-20 SpecTech Universal

Although it can be seen that the equipment string is relatively complex and the calibration can be tedious and difficult, it is still necessary to evaluate the overall performance of the boron trifluoride detector itself.

a. Experimentation and Analysis

Once the equipment was set up and powered on in the laboratory environment, it was first necessary to calibrate the detector and find the background levels of radiation before readings with individual neutron sources could take place. In order to calibrate the detector, a Pu-Be neutron source was placed under the aluminum tube, and the reading on the UCS30 software was compared to the expected pulse height spectra from BF_3 tubes. The expected pulse height spectra can be seen in Figure 12.

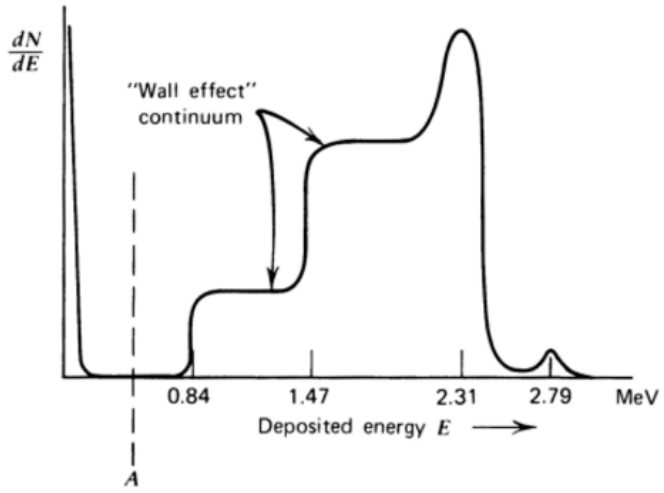

Figure 12. Expected pulse height spectra from BF_3 tubes, with noted continuum due to wall effect. Adapted from [5].

Therefore, an initial calibration reading was taken using the UCS30 software, and the gain was appropriately adjusted to ensure that the expected pulse height spectra showed discernible steps, most notably at the expected peaks of roughly 2.31 MeV and 2.79 MeV. Figure 13 shows the result of the properly configured gain settings that were achieved to allow for actual measurements of neutron source detection.

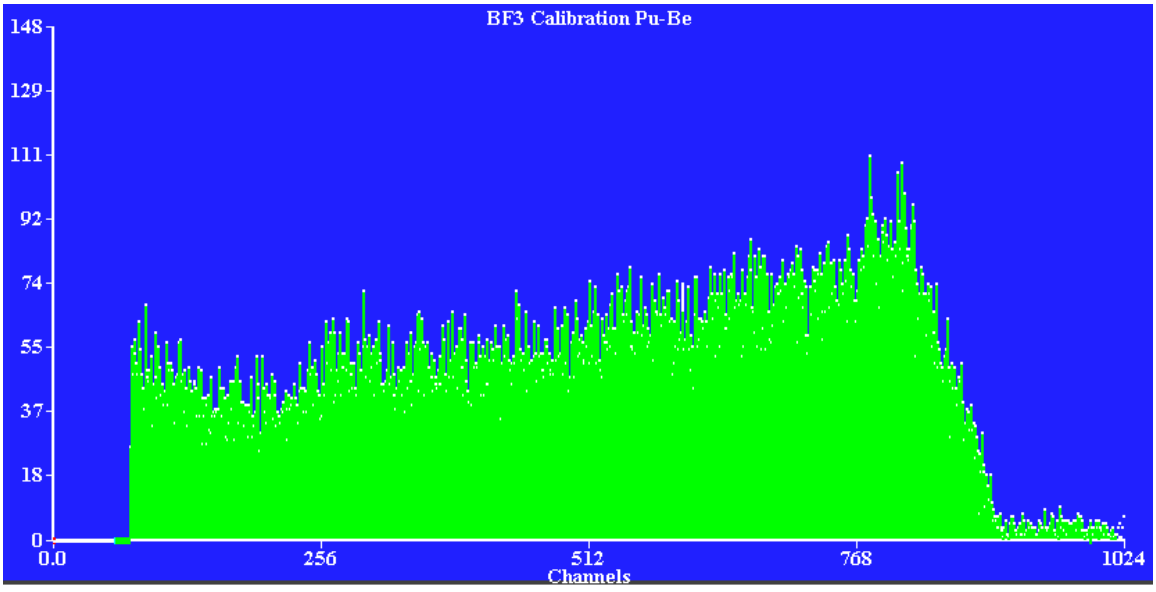

Figure 13. Pulse height spectra achieved while calibrating BF_3 detector using a Pu-Be source.

Once the calibration was complete, it was time to find the background readings for the detector over the course of 30 minutes. Since the Pu-Be source has a much higher activity than that of Cf-252, it was determined that the Pu-Be source would take readings for only 5 minutes, and the Cf-252 source would take readings for 30 minutes. The background readings were taken without any source present over the course of 30 minutes, and the number of counts was determined to be 24. Therefore, the background counts for the Cf-252 readings would be 24, and the background counts for the Pu-Be readings would be 24*(5/30), or 4 counts.

After calibration and background measurements were complete, it was time to take neutron detection readings with the boron trifluoride detector using the Pu-Be and Cf-252 sources. This was done using similar methodology to what was used to analyze the NE-213 liquid scintillator. Initially, a Cf-252 source was placed at a distance of 50 cm from the detector, and the detector registered neutron counts over the course of 30 minutes. This was process was then repeated at a distance of 100 cm. After the data for these two readings was logged, the next step was to repeat the process using Pu-Be at the same distances, for a time of 5 minutes at each distance. Once the data was taken, the next step was to calculate the detector efficiency for each of the readings, which can be seen in Table 18.

Table 18. Experimental data and intrinsic neutron detection efficiency results for BF_3 detector using Cf-252 and Pu-Be sources.

Source	Distance (cm)	Time (s)	Gross Counts	Background Counts	Background Subtracted Gross Counts	Neutrons Counted Per Second	Fluence (neutrons/cm^2/sec)	Cross-sectional Detector Area (cm^2)	Total Neutrons Through Sensitive Volume (neutrons/s)	Intrinsic Detection Efficiency
Cf-252	50	1800	912	24	888	0.49	2.054856	29.0322	59.66	0.83%
Cf-252	100	1800	415	24	391	0.22	0.513714		14.91	1.46%
Pu-Be	50	300	6,991	4	6,987	23.29	70.028175	29.0322	2033.07	1.15%
Pu-Be	100	300	1,774	4	1,770	5.90	17.507044		508.27	1.16%

As can be seen in Table 18, the first step in this process was to subtract the background counts from the gross counts registered by the UCS30 software for each experiment. The result of this was the background subtracted gross counts, and dividing this by the time duration of each experiment (1800 seconds or 300 seconds) resulted in the value for neutrons counted per second. By comparison, the fluence was calculated using the same process as was described in the NE-213 liquid scintillator analysis, utilizing the formula

$$\Phi = \frac{N}{4\pi d^2}.$$

This time, however, the *N* value for the Cf-252 source was not 17447.3 fissions per second. Since the BF_3 detector is only measuring neutrons, this value was multiplied by 3.7 fissions per second (the accepted value for Cf-252), which results in a total *N* value of 64555.2 neutrons per second [14]. The *d* value was again varied between 50 cm and 100 cm, depending on which distance the neutron source was from the detector for that particular measurement. The fluence was then multiplied by the cross-sectional area of the aluminum tube of the detector to obtain the value for neutrons per second through the sensitive volume of the detector. The length of the aluminum tube is 6 inches, and the diameter is 0.75 inches, which results in a cross-sectional area of 4.75 in^2. Converted into cm^2, the resulting cross-sectional area is 29.0322 cm^2. Once the value for neutrons per second through the sensitive volume of the detector was calculated, dividing the neutrons per second registered by the detector by this value resulted in the intrinsic detection efficiency for each experiment.

For the californium-252 source, the detection efficiency of the BF_3 detector was found to be 0.83% of incident neutrons at a distance of 50 cm, and 1.46% of incident neutrons at a distance of 100 cm. For the plutonium-beryllium source, the detection efficiency of the BF_3 detector was found to be 1.15% of incident neutrons at a distance of 50 cm, and 1.16% of incident neutrons at a distance of 100 cm. At best, the BF_3 detector is then only capturing 31.3% of the amount of neutrons that the NE-213 liquid scintillator was able to detect from the Cf-252 source, making the NE-213 approximately 3.2 times

more efficient. For the Pu-Be source, the BF_3 detector was only able to detect about 9% of the neutrons that the NE-213 was able to register, making the NE-213 detector 11.1 times more efficient.

b. Conclusions

Compared to the Beckman LS 6500 Scintillation System and the NE-213 liquid scintillator, the boron trifluoride detector has a slightly simpler equipment string, and is easier to calibrate than a NE-213 detector. Although its equipment string is slightly less complex than a NE-213 liquid scintillator, the BF_3 detector was found to be much less efficient at fast neutron detection. For a Cf-252 source, the NE-213 was able to detect up to 8.47% of incident neutrons at 50 cm, and up to 9.87% of incident neutrons at a distance of 100 cm. Comparatively, the BF_3 detector was only able to detect 0.83% of incident neutrons at 50 cm and 1.46% of incident neutrons at 100 cm. For a Pu-Be source, the NE-213 was able to detect up to 15.98% of incident neutrons at 50 cm, and up to 16.97% at a distance of 100 cm. Comparatively, the BF_3 detector was only able to detect 1.15% of incident neutrons at 50 cm and 1.16% at a distance of 100 cm. Overall, the NE-213 liquid scintillator had a more complex equipment string, was more difficult to calibrate, and required sweeping through various PSD settings to find a peak detection efficiency. Conversely, the BF_3 detector had a simpler equipment string, easier calibration, and did not require PSD adjustments, but was much less efficient at detecting incident neutrons.

III. CENTRIFUGAL TENSIONED METASTABLE FLUID DETECTOR

A. THEORY

The following research investigates the centrifugal tensioned metastable fluid detector (CTMFD), a technology that promises a compact, easy to use, highly sensitive, robust, discriminatory, mobile sensor platform for detection of the presence of special nuclear materials in real time. Unlike the detectors previously discussed in this work, the CTMFD operates using only a computer connected to three pieces of equipment. CTMFDs are also blind to beta and gamma radiation, and can be procured at a fraction of the price of other current, more expensive, immobile detectors. If proven effective, CTMFDs could provide significant assistance to governmental agencies throughout the world, and specifically the U.S. Department of Defense, in detecting trace amounts of special nuclear material or other source materials in transit or on the battlefield. The CTMFD provides two unique capabilities: real-time, low-cost thermal and fast neutron detection, and alpha spectroscopy (specifically of actinides).

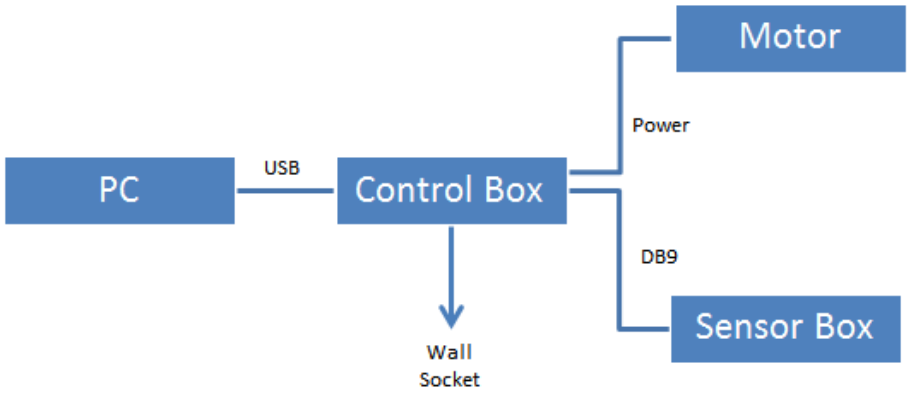

Figure 14. Visual layout of equipment string used for CTMFD during the conduct of this research.

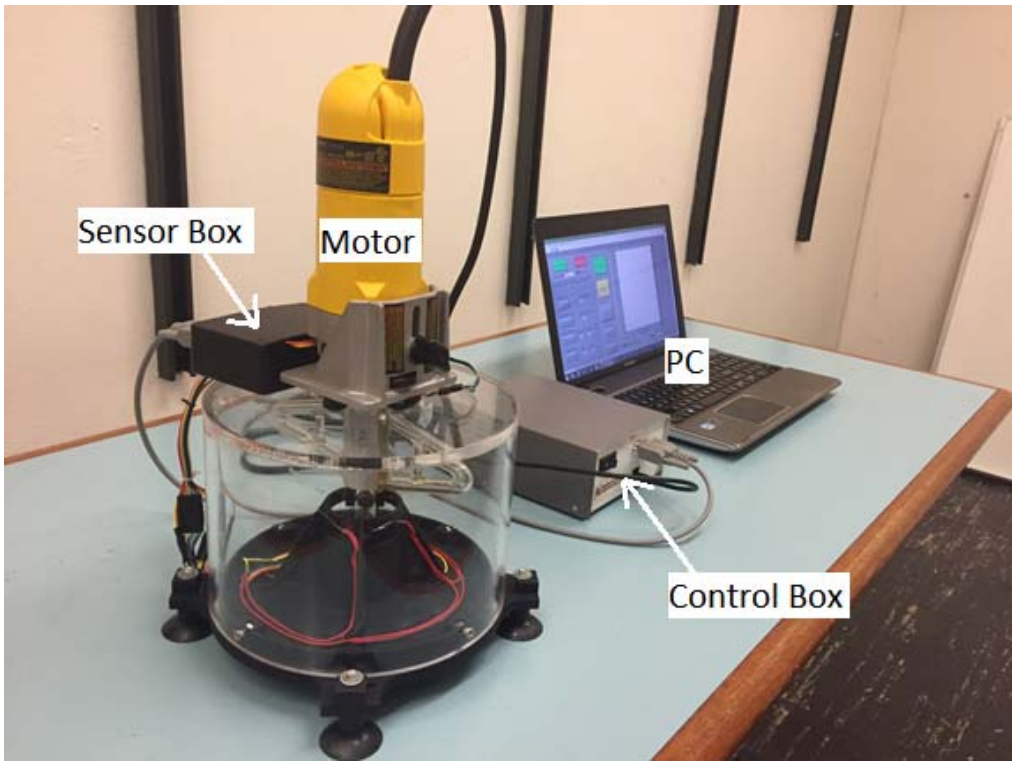

Figure 15. Photograph of CTMFD and associated equipment used during the conduct of this research.

Contrasting other detectors used in the conduct of this research up to this point, the CTMFD has a simpler equipment string that makes it much more mobile, hardy, and cheaper to produce. As can be seen in Figures 14 and 15, a laptop is simply connected to a control box, which in turn is connected to a motor and sensor box that are bolted together. This lack of a complex equipment string makes the detector much more mobile, and arguably simpler to operate and maintain than other detectors with similar capabilities.

1. Working Scientific Principles

The principle behind the CTMFD is to utilize various amplitudes of centrifugal force to obtain tensioned metastable states in a working liquid, and then use this liquid as the detector medium. The working liquid (acetone or decafluoropentane) is placed within the glass bulb of the detector, which is then rotated by a drill motor at a speed controlled by the computer software. The faster the bulb rotates, the higher the amplitude of the

negative pressure inside the bulb, and thus the higher tension of the fluid. As the tension of the fluid increases and moves away from stability limits, additional energy added to the system by an ionizing particle triggers a phase change. When an ionizing particle such as a (fast or thermal) neutron or alpha particle is absorbed by the liquid, energy stored within the liquid is freed through vaporization growth of fast nucleating vapor bubbles. If the initial energy deposited into the liquid is high enough, a critical size vapor nucleus will be created (in the nanometer range). Higher tension of the fluid inside the detector bulb means less energy is needed from the ionizing particle to create a critical-size vapor nucleus. In other words, when measuring for ionizing particles of lower energy, a higher tension is needed and therefore the drill motor needs to rotate the bulb more quickly than if trying to detect higher energy particles. Once the newly created vapor nucleus grows into a macroscopic bubble, there is a distortion in light transmission in the detector bulb that is distinguished by a sensor in the bottom of the detector. Within a matter of seconds, the bubble will also burst and create an audible “pop” sound that can be detected by the human ear. These two events signal a registered detection of an alpha particle or neutron. Figure 16 shows a visual representation of the detector bulb within the CTMFD.

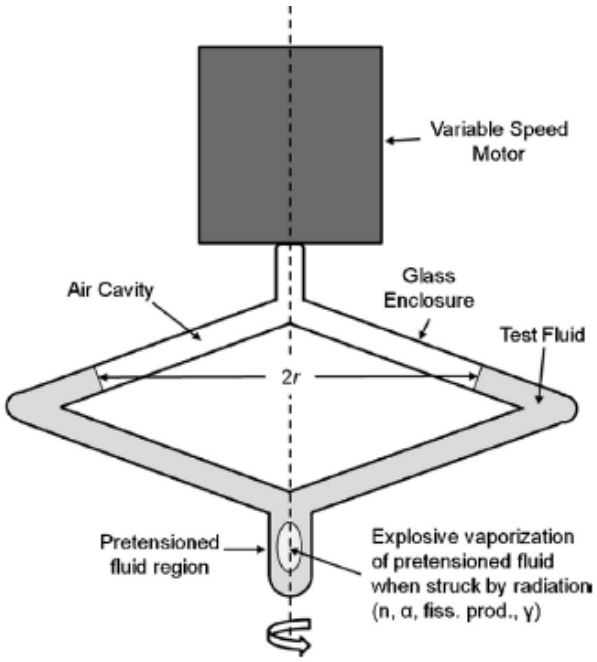

Figure 16. Schematic representation of CTMFD detector bulb and working principles. Adapted from [3].

In order to calculate the value of negative pressure within the sensitive volume of the bulb, the well-known Bernoulli equation is used:

$$P_{neg} = 2\pi^2 \rho \left(r - r'\right)^2 f^2 - P_{amb},$$

where P_{neg} is the value for negative pressure, ρ is the density of the working liquid, r is the radius from the centerline of the bulb to the meniscus, $r'$is 0 (since the point of interest is at the centerline of the detector), f is the rotational speed of the bulb (in rotations per second), and P_{amb} is the ambient pressure. The calculations for the negative pressure are all done by the computer software, given the user inputs of the ambient temperature, type of working fluid, and the diameter of the fluid meniscus. Based on previous studies, the CTMFD was able to detect 1–5 MeV neutrons and alpha particles at modest negative pressures (-7 to -9 bar) [3].

a. Detection of Fast Neutrons

During the process of neutron detection, the bulb is filled with a working fluid (acetone or decafluoropentane) and screwed into the base of a drill motor, which is

controlled by a laptop running the detector software. Based on the desired sensitivity range, the user controls the speed of the drill motor using the computer software. The higher the rotational speed of the bulb attached to the drill, the higher the amplitude of negative pressure inside of the bulb, and the more sensitive the detector becomes to neutrons of lower energy. Once the detector is set up, the neutron source is placed within the desired distance of the detector bulb. When a neutron of the appropriate energy strikes the pretensioned fluid, explosive vaporization occurs which creates a bubble inside of the bottom of the bulb, which quickly produces an audible "pop." A light-sensitive sensor inside of the detector notices the adjustment in light reflecting off the bubble inside of the bulb, and stops the detector. Based on the computer software's instructions, the detector will wait 1–2 minutes for the system to cool down, and will then spin the drill up to the desired speed again in order to provide the desired pressure inside the bulb. All of the recorded time, pressure, and error limit data is kept within the computer software and can be exported to an Excel spreadsheet. Based on the average time it takes for a bubble to be created at a given pressure (sensitivity), it is possible to differentiate between fission sources and a random neutron source.

b. Alpha Particle Spectroscopy of Actinides

The second capability of the CTMFD is alpha spectroscopy, which involves a slightly different setup, specifically within the detector bulb. Since alpha particles are relatively massive, they generally do not travel very far in air and therefore often cannot be detected even within close range of the source. To combat this issue, the source is placed in a measured solution with acetone or decafluoropentane inside of the detector bulb itself. This is different than the execution of neutron detection, where the source is outside of the detector as was seen in the NE-213 and BF_3 detector experiments. Again, the bulb is spun by the drill motor from the computer software to a designated speed, according to the desired pressure and therefore sensitivity inside of the detector. As before, the higher the rotational speed of the bulb, the higher the sensitivity to lower energy alpha particles. Once spun up to a proper speed and pressure, an alpha particle that is emitted from the source inside the bulb will strike the molecules of the pre-tensioned fluid, creating explosive vaporization and a bubble that is noticed by the sensor

inside of the detector. Based on the average time it takes for a bubble to be created at a given pressure (sensitivity), the source can be differentiated between isotopes such as Pu-238, Pu-239, and UN.

B. EXPERIMENTATION AND RESULTS

1. Detection of Fast Neutrons

In order to test the efficiency of the centrifugal tensioned metastable fluid detector for detecting neutrons, the detector and associated equipment were set up, and testing was done with two separate neutron sources at various distances. Before the testing could begin, the detector bulb was filled with decafluoropentane and the distance between the meniscuses at the ends of the bulb were measured. This measurement was entered into the detector software, and decafluoropentane was selected within the software as the working fluid. Once the detector bulb was screwed back into the drill motor and all CTMFD equipment was secured, the first neutron source was brought out. Cf-252 was placed 50 cm away from the center of the bulb, and at a level even with the height of the bulb itself.

Once the experimental setup was ready, the next step was to run the detector and begin taking measurements of the wait time for a bubble to form at various negative pressures. Based on previous studies done at Purdue University, it was determined that a good starting point for neutron detection is in the -4 bar range [15]. The detector software was set up to run automatically: spinning the motor and maintaining a -4 bar pressure level, recording and averaging the time it took for a detection to be registered, and allowing the drill motor to cool for 60 seconds in between detections. If a detection was not registered within 60 seconds, the computer software stopped the drill motor for 60 seconds to prevent the system from overheating.

The first experimental data taken involved a Cf-252 source at a distance of 50 cm from the CTMFD bulb. At -4 bar, 62 detections were registered over a detector run time of 424.57 seconds, which translates to an average wait time of 6.85 seconds. The pressure was then brought down to -3 bar using the computer software, to determine if the detector system would become less sensitive as expected. After 50 detections over a time of

1551.78 seconds, the average wait time at a pressure of -3 bar was found to be 31.04 seconds. This is consistent with the detection theory of the CTMFD. Next, the Cf-252 sources were removed from the experimental area, and a Pu-Be source was placed at a distance of 500 cm from the detector (the distance was increased since Pu-Be has a higher activity than Cf-252). For this source and distance from the detector, the negative pressures used by the CTMFD were the same to allow for comparison to the Cf-252 source measurements. The first negative pressure used for this portion of the test was -4 bar, at which the CTMFD registered 50 detections over a total run time of 317.3 seconds. This translates to an average wait time of 6.35 seconds. At -3 bar, the detector registered 49 detections over a total run time of 772.72 seconds, averaging a wait time of 15.77 seconds between detections. Table 19 shows the intrinsic detection efficiency values based on calculations from the average wait time as discussed previously.

Table 19. Experimental data and intrinsic neutron detection efficiency results for CTMFD using Cf-252 and Pu-Be sources.

Source	Distance (cm)	Fluence (neutrons/cm^2/sec)	Cross-sectional Detector Area (cm^2)	Total Neutrons Through Sensitive Volume (neutrons/s)	Pneg (bar)	Average Waiting Time (s)	Detection Rate (cps)	Intrinsic Detection Efficiency
Cf-252	50	2.054856	7.0	14.38399086	4.0	6.85	0.145985	1.01%
Cf-252	50	2.054856	7.0	14.38399086	3.0	31.04	0.032216	0.22%
Pu-Be	500	0.700282	7.0	4.901972247	4.0	6.35	0.15748	3.21%
Pu-Be	500	0.700282	7.0	4.901972247	3.0	15.77	0.063412	1.29%

The fluence was again calculated using the formula

$$\Phi = \frac{N}{4\pi d^2},$$

using the same *N* values as were determined in the calculation for the BF_3 detector (since the CTMFD is gamma-blind). The cross-sectional area of the bulb used during this research is 7.0 cm^2. The total neutrons through the sensitive volume is then found by multiplying the fluence by the cross-sectional area, and the detection rate (in counts per second) is found by taking the inverse of the average waiting time that was acquired in the experimental data. Dividing the detection rate by the total neutrons per second through the sensitive volume of the detector results in the value for intrinsic neutron detection efficiency. For the Cf-252 source, the CTMFD was found to have a 1.01% detection efficiency at -4 bar and a 0.22% efficiency at -3 bar. The experimentation with the Pu-Be source at 500 cm found that the CTMFD had a 3.21% detection efficiency at -4 bar, and a 1.29% efficiency at -3 bar.

2. Alpha Particle Spectroscopy of Actinides

The second capability of the centrifugal tensioned metastable fluid detector is the ability to discriminate between different isotopes of uranium and plutonium using alpha particle spectroscopy. This study has previously determined that the Beckman LS 6500 Scintillation System was able to discriminate between stock (highly concentrated) solutions of Pu-238, Pu-239, UN, and background levels. However, the Beckman LS 6500 failed at discriminating between the solutions and background levels when the stock solutions were diluted to ~1% of original concentration. In order to test the CTMFD against the capabilities of the Beckman system, similarly diluted solutions were utilized in the CTMFD experimentation.

a. Plutonium Experimentation and Analysis

The first step in the process was to utilize the solutions that were created for use with the CTMFD and the Beckman LS 6500 Scintillation System, as listed in Table 3. These solutions were created with an appropriate activity as to expect a 10-second

waiting time for detection by the CTMFD. First, the Pu-238 solution was placed into the bulb of the detector, and then a series of tests was completed from 7.75 bar to 8.75 bar, in increments of 0.25 bar. Next, the bulb was thoroughly rinsed with acetone filled with the Pu-239 solution that was created with an expectation of a 10-second wait time for detection by the CTMFD. Using the automated computer software, testing was done from 7.25 bar to 8.5 bar, in increments of 0.25 bar. The results of these initial tests, and the expected wait time that emerged for each pressure level, can be seen in Table 20. Table 20 also shows the error limits as calculated by the CTMFD software.

Table 20. Experimental data of average detection wait time at various negative pressures using CTMFD and original Pu-238 and Pu-239 solutions.

Isotope	Pneg (bar)	Wait time (s)	Error
Pu-238 (0.03 Bq/g)	7.75	107.21	32.33
	8.00	55.94	16.87
	8.25	41.13	10.62
	8.50	47.10	10.53
	8.75	39.81	6.29
Pu-239 (0.03 Bq/g)	7.25	67.76	14.45
	7.50	30.00	5.67
	7.75	18.08	3.69
	8.00	14.49	2.96
	8.25	15.65	3.34
	8.50	10.31	2.37

Unexpectedly, the average wait time for Pu-238 was much higher than the 10-second wait time that was anticipated based on the initial calculations for the solution. This was likely due to the fact that the detector only had 60 seconds to cool down in between detections, or possibly because the solution was not as radioactive as was originally measured. In order to combat this, a new solution was created that would roughly achieve the 10-second wait time to allow for comparisons between the isotopes. Since the expected wait time initially determined was roughly four times higher than expected (specifically at least 39.81 seconds as seen in Table 20), a new Pu-238 solution

was created using approximately four times more stock solution than the original diluted solution (see Table 25 in the Appendix for specific masses). Also, the wait time in between detections was increased to 120 seconds in order to allow more time for the drill motor to cool, and the temperature compensation setting was enabled on the detector software. This would allow the detector to calculate the temperature of the fluid, and adjust the density of the fluid as entered into Bernoulli's equation. Utilizing this new solution for Pu-238, and the new delay and temperature settings for the CTMFD itself, a new set of tests was run utilizing the same pressure increments from the previous test. For the sake of thoroughness, the detector bulb was then rinsed, and the original Pu-239 solution was used in the bulb so that new data could also be obtained for this solution using the new temperature and delay settings. The new experimental data can be seen in Table 21.

Table 21. Experimental data of average detection wait time at various negative pressures using CTMFD and new Pu-238, original diluted Pu-239 solutions, with improved temperature settings.

Isotope	Pneg (bar)	Wait time (s)	Error
Pu-238 (0.12 Bq/g) 120s Restart Time Temp. Comp at Run Start	7.25	123.09	35.53
	7.50	33.84	7.57
	7.75	35.38	7.91
	8.00	15.04	2.70
	8.50	11.41	2.55
Pu-239 (0.03 Bq/g) 120s Restart Time Temp. Comp at Run Start	7.25	121.56	60.78
	7.50	42.47	9.27
	7.75	21.04	4.71
	8.00	13.92	3.11
	8.50	6.60	1.48

As can be seen in the data in Table 21, this updated solution along with adjusted temperature settings made the expected wait time much closer to the expected value of 10 seconds. However, neither the Pu-238 nor the Pu-239 solution had a value for an expected wait time that was exactly 10 seconds, so the data was normalized around an exact 10-second wait time for the sake of effective comparison. This was done by

multiplying the Pu-238 solution wait times by (10/11.41), and the Pu-239 solution wait times by (10/6.60). The resulting wait times normalized around a 10-second detection time can be seen in Table 22, and will serve as the final data points for the Pu solutions.

Table 22. Normalized values of average detection wait time at various negative pressures using CTMFD and new Pu-238, original diluted Pu-239 solutions, with improved temperature settings.

Isotope	Pneg (bar)	Wait time (s)	Error
Pu-238	7.25	107.88	31.14
	7.50	29.66	6.63
	8.00	13.18	2.37
	8.50	10.00	2.23
	7.75	31.01	6.93
Pu-239	7.25	184.18	92.09
	7.50	64.35	14.05
	7.75	31.88	7.14
	8.00	21.09	4.71
	8.50	10.00	2.24

In order to determine whether or not the CTMFD was able to discriminate between the Pu-238 and Pu-239 solutions, the values of wait time vs. negative pressure were plotted graphically. As can be seen in Figure 17, the average wait time for Pu-238 is consistently below that of Pu-239, even with error bars taken into consideration. It should be noted that with similarly diluted solutions, the Beckman LS 6500 Scintillation System was unable to discriminate between these two plutonium solutions and background levels. Figure 17 shows that the CTMFD is indeed able to discriminate between the two highly diluted solutions.

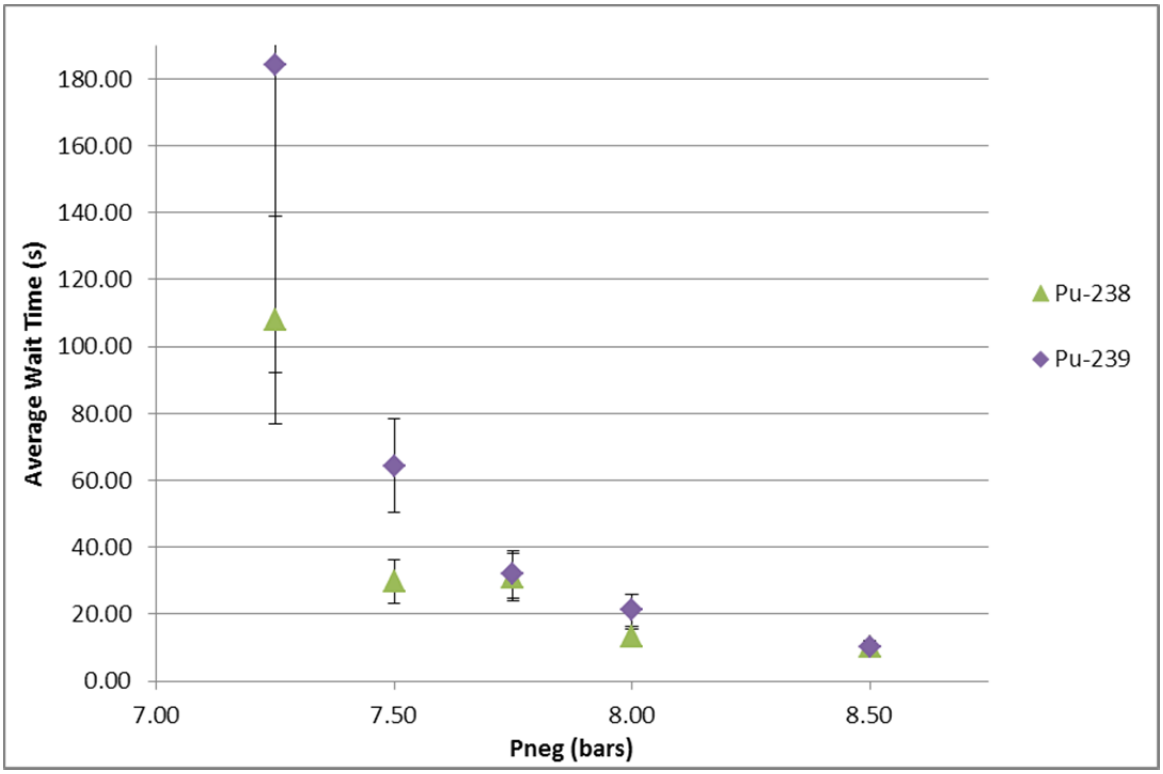

Figure 17. Plot of normalized average wait time vs. negative pressure for Pu-238 and Pu-239 solutions which proves the alpha spectroscopy capabilities of the CTMFD.

b. Uranyl Nitrate Experimentation and Analysis

The final step for verifying the actinide spectroscopy capabilities of the centrifugal tensioned metastable fluid detector was to perform experimentation with UN solution in a similar manner as was conducted for the Beckman LS 6500 Scintillation System. Similar to how the original Pu-238 and Pu-239 solutions were created, a UN solution was created with an activity that would be expected to create a 10-second wait time for the CTMFD. This study previously proved that this diluted solution could not be detected by the Beckman LS System, and the specifics for the solution can be found in Table 9 of this work.

In order to ensure that this diluted solution could be detected in a time of approximately 10 seconds, the solution was placed in the bulb of the CTMFD, and the software set for a negative pressure of 10.5 bar. After 7 detections, the wait time was found to be higher than expected, at 55.67 seconds. In order to compensate for this and

facilitate a 10-second wait time that would allow for comparison with the Pu isotopes, a new solution was created with an estimated six times higher calculated specific activity (roughly 0.18 Bq/g, see appendix for specific masses). After the bulb was thoroughly rinsed with acetone, this new solution of higher activity was placed in the bulb with a syringe. Utilizing the CTMFD software, pressure readings were taken and logged at negative pressures of 7.5, 7.75, 8.0, 8.5, and 9.0 bar. The average detection times of the readings at each individual pressure can be seen in Table 23.

Table 23. Experimental data of average detection wait time at various negative pressures using CTMFD and new UN solution.

Isotope	Pneg (bar)	Wait time (s)	Error
UN (0.18 Bq/g)	7.50	141.44	44.73
120s Restart Time	7.75	76.93	15.7
Temp Comp at Run Start	8.00	7.13	2.52
	8.50	7.91	1.82
	9.00	5.76	1.54

As can be seen in Table 23, this updated solution provided for an average wait time much closer to the expected wait time of 10 seconds. Since Pu-238 and Pu-239 have similar alpha decay energies, they were normalized at the same negative pressure (8.5 bar), but UN has a lower energy alpha decay, and therefore required a higher negative pressure to plateau (9.0 bar). In order to allow for a more exact comparison of the expected wait times between isotopes, the UN wait times seen in Table 23 were normalized around a 10-second wait time for a negative pressure of 9.0 bar. This was done by multiplying the UN solution wait times by (10/5.76). The resulting wait times normalized around a 10-second detection time at -9.0 bar can be seen in Table 24, and will serve as the final data points for the UN solution.

Table 24. Normalized values of average detection wait time at various negative pressures using CTMFD and new UN solution.

Isotope	Pneg (bar)	Wait time (s)	Error
UN (0.18 Bq/g)	7.50	245.56	77.66
120s Restart Time	7.75	106.85	27.26
Temp Comp at Run Start	8.00	12.38	4.38
	8.50	13.73	3.16
	9.00	10.00	2.67

Now that normalized wait times have been established for the Pu-238, Pu-239, and UN solutions, it is time to analyze and compare the three graphically. As can be seen from Figure 18, there is a visible difference in the drop off of the slope of the wait time versus negative pressure curve between each of the three isotopes. The Pu-238 solution initially has the lowest average wait time, and plateaus around -7.5 bar. The Pu-239 has the next highest average wait time at the lower negative pressures, and begins a gentle sloped plateau around -7.75 bar. Finally, the UN solution has the highest initial average wait time, and does not begin to plateau until -8.0 bar, at which point it remains almost completely flat. This confirms previous work by Taleyarkhan et al., and proves that the CTMFD can indeed discriminate between diluted Pu-238, Pu-239, and UN sources, unlike the Beckman LS 6500 Scintillation System which could not even discriminate between the diluted solutions and background levels [3].

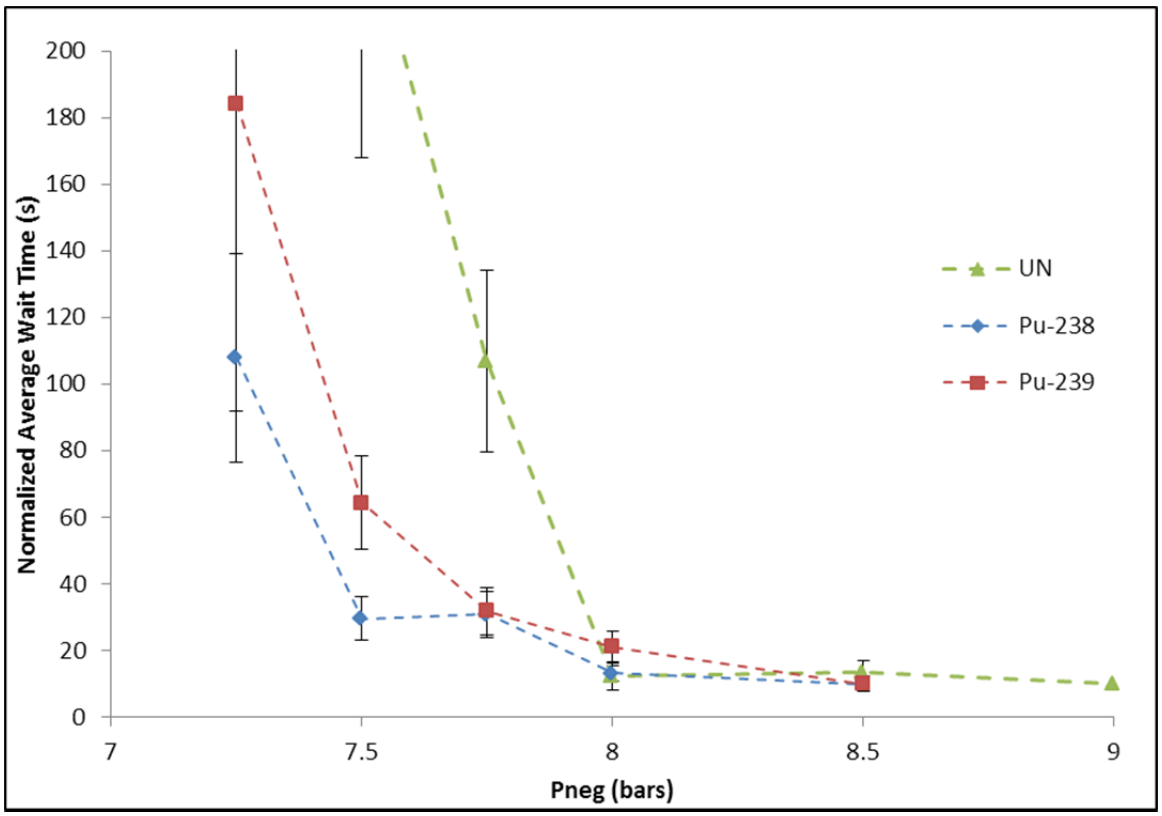

Figure 18. Plot of normalized average wait time vs. negative pressure for Pu-238, Pu-239, and UN solutions which proves the alpha spectroscopy capabilities of the CTMFD.

3. Conclusions

The centrifugal tensioned metastable fluid detector uses a simple equipment string and a pressurized working fluid to provide both detection of fast neutrons as well as alpha particle spectroscopy. In order to test its neutron detection capabilities, neutron sources were placed a measured distance from the detector bulb, which was filled with acetone and spun up to various negative pressures. Using a Cf-252 source at a distance of 50 cm, the CTMFD was found to detect 1.01% of neutrons passing through the sensitive volume of the detector. For a Pu-Be source at a distance of 500 cm from the detector, the CTMFD was found to detect up to 3.21% of neutrons passing through the sensitive volume of the detector. The second capability of the CTMFD is discrimination of actinide sources using alpha particle spectroscopy. Testing was done utilizing similarly diluted solutions of Pu-238, Pu-239, and UN that were unable to be detected by the Beckman LS

6500 Scintillation System. The original diluted solutions of Pu-238 and UN were not as close to their projected average wait time of 10 seconds as expected, so their activities were slightly increased proportionally based on the actual wait times. Once all three solutions had been tested over multiple negative pressures, a negative pressure value that was proportional to the decay energy was used to normalize the remaining wait times around an average of a 10-second wait time. This data was then plotted graphically, and there was a noted difference in the plateaus of average wait time versus negative pressure for all three solutions. In other words, the CTMFD was not only able to detect the alpha particles in all three of the solutions, but it was also able to discriminate between the three solutions individually. This is a marked advantage over the Beckman LS 6500 Scintillation System, which was unable to even detect the presence of any radioactivity in these solutions as compared to background levels.

THIS PAGE INTENTIONALLY LEFT BLANK

IV. CONCLUSIONS

A. SUMMARY OF SCIENTIFIC FINDINGS

In addition to the centrifugal tensioned metastable fluid detector, three other detectors were utilized in this study which had comparable capabilities to those of the CTMFD. The first was the Beckman LS 6500 Scintillation System, which was used to compare to the alpha spectroscopy capabilities of the CTMFD. The Beckman LS System was easily able to discriminate between highly concentrated solutions of Pu-238, Pu-239, and UN. However, once the stock solutions were diluted to roughly 1% of the original activity level, the Beckman LS System was unable to detect the presence of any of these three solutions against background levels. The CTMFD, on the other hand, was not only able to detect the presence of highly diluted solutions of Pu-238, Pu-239, and UN, but was also able to discriminate between the three separate solutions based on the position of the plateau on the average wait time versus negative pressure curve.

Further, the NE-213 liquid scintillator and the boron trifluoride detector were also analyzed in order to compare neutron detection capabilities with that of the CTMFD. Although the NE-213 had a complex equipment string and was difficult to calibrate, it was able to detect up to 8.47% and 9.87 % of incident neutrons from a Cf-252 source at a distance of 50 cm and 100 cm, respectively. For a Pu-Be source, the NE-213 detected up to 15.98% of incident neutrons at a distance of 50 cm from the source, and 16.97% of incident neutrons at a distance of 100 cm from the source. Next, a boron trifluoride detector was set up and used to detect neutrons from a Cf-252 and Pu-Be source at 50 cm and 100 cm. Although the equipment string of the BF_3 detector was simpler than that of the NE-213, it was found to be much less efficient at detection of incident neutrons. The BF_3 was able to detect only 0.83% of incident neutrons at a distance of 50 cm from a Cf-252 source, and 1.46% at a distance of 100 cm from the Cf-252 source. Using a Pu-Be source, the BF_3 detector was found to detect only 1.15% of incident neutrons at a distance of 50 cm from the source, and 1.16% at a distance of 100 cm from the source. Finally, neutron detection was done using these same neutron sources and a centrifugal tensioned metastable fluid detector, which has a much simpler equipment string than any of the

other detectors used in this research. At a distance of 50 cm from a Cf-252 source, the CTMFD was found to have up to a 1.01% detection efficiency of incident neutrons at the negative pressures that were tested. For a Pu-Be source at a distance of 500 cm, the CTMFD was found to have a detection efficiency of up to 3.21%. In other words, at a distance of 50 cm from a Cf-252 source, the CTMFD was found to be more efficient than a boron trifluoride detector, but much less efficient than a NE-213 liquid scintillator at fast neutron detection. Figures 19 and 20 show plots of the detection efficiency of the CTMFD as compared with the NE-213 and BF_3 detectors at various distances, utilizing Cf-252 and Pu-Be sources.

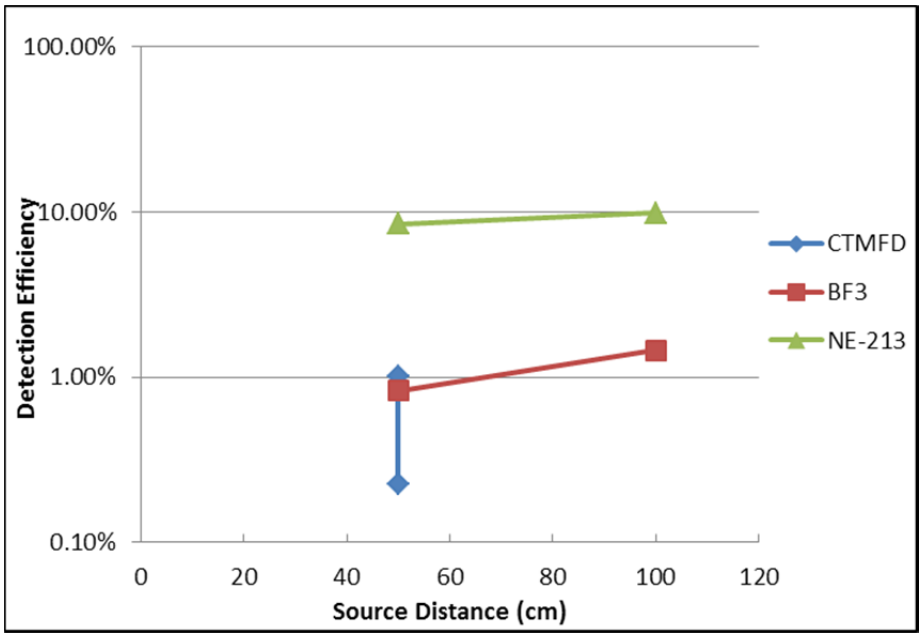

Figure 19. Plot of neutron detection efficiency of selected detector types using Cf-252 source at various distances.

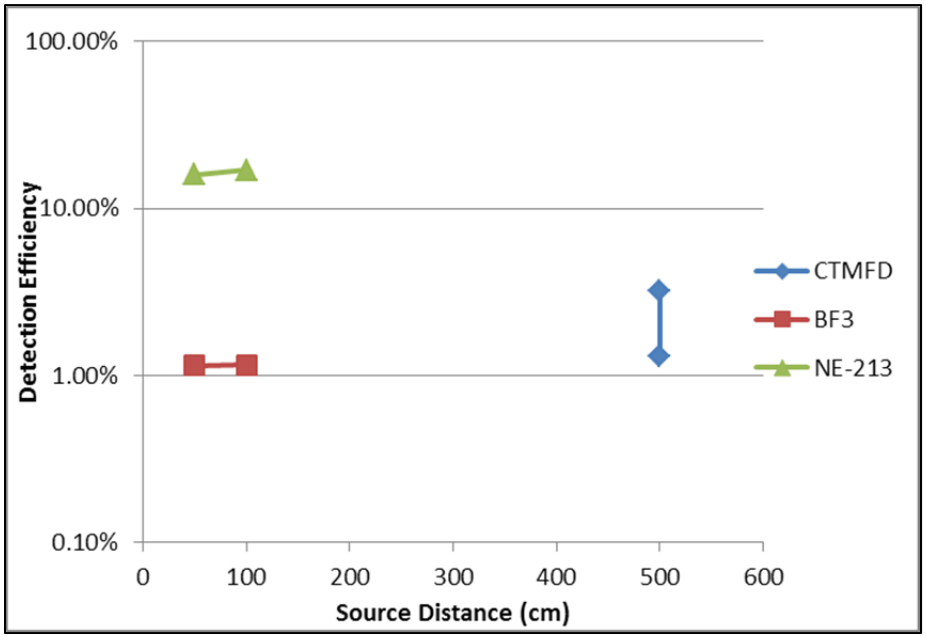

Figure 20. Plot of neutron detection efficiency of selected detector types using Pu-Be source at various distances.

B. RECOMMENDATIONS FOR CTMFD USE

The primary advantage of the CTMFD as compared with the Beckman LS 6500 Scintillation System, NE-213 liquid scintillator, and boron trifluoride detector is the fact that the CTMFD's equipment string is much more minimalistic. Utilizing just three main components, the CTMFD can be moved, setup, and powered on in a quick and efficient manner. Although it was proven to be less efficient than a NE-213 detector at neutron detection, the CTMFD was still able to detect up to 3.21% of incident neutrons from a Pu-Be source at a distance of 5 meters. With more research on various (likely increased) negative pressures, the CTMFD could become an effective tool at interrogating potential sources of fast neutrons (nuclear weapons) at military checkpoints. However, due to its need to cool off every 60 seconds, multiple detectors would have to be used in overlapping time sequences. Also, since the detector is generally only sensitive to certain ranges of particle energies depending on the negative pressure of its working fluid, multiple detectors would also need to be used to sweep at various sensitivities. Considering the fact that each detector can be produced on the order of hundreds of dollars, fielding multiple detector units in one location is still likely cheaper than using

any of the other detector options utilized in this research. Also, scanning across multiple energy levels may provide a spectroscopy capability for fast neutron sources in real time.

The CTMFD was also found to be extremely effective at actinide spectroscopy, detecting and discriminating amongst actinide solutions of low concentration that could not even be detected by a Beckman LS 6500 Scintillation System. Therefore, the CTMFD could be an effective tool in DOD's mission to aid in domestic or foreign consequence management situations in the wake of a nuclear attack. A single detector could be flown out to the disaster area quickly and easily, and utilizing some material from a collected radioactive source, the isotopes could be determined after sweeping through several negative pressures and determining the plateau of the wait time versus negative pressure plot. The detector could also be used in situations that do not involve post-detonation analysis, including interrogating parts of a source from a nuclear weapon before it is detonated to aid in determining its origin.

C. RECOMMENDATIONS FOR FUTURE RESEARCH

Although the CTMFD has already proven to be a useful and cost-effective tool in the areas of neutron detection and actinide spectroscopy, further research could help to understand how to make it more beneficial in a military environment. Experimenting with various bulb sizes and pressure ranges, and building data tables that specify expected wait times for various isotopes could provide CTMFD users with quick access to predict which sources they might be interrogating. This would also prevent the user from having to conduct time-consuming sweeps at a large amount of negative pressures. Further, constructing a CTMFD that uses multiple bulbs as part of one detector, or creating software that can run multiple CTMFDs at once, could make the CTMFD design easier to use, more cost-effective than multiple individual detectors, and more effective at interrogating radioactive sources in a military environment.

Another promising potential capability of the CTMFD is the potential to provide specific neutron spectroscopy capabilities. Since the principle detection mechanism of the CTMFD allows it to detect a single neutron, the detector could theoretically be used to detect neutrons of relatively low energies, or provide the capability to effectively read the

energy of an incident neutron. Future work could involve conducting research to detect the minimum energy threshold for neutron detection, and finding the specific ranges of neutron energies that could be detected for specific negative pressures.

THIS PAGE INTENTIONALLY LEFT BLANK

APPENDIX. ADDITIONAL DATA

Table 25. Mass values measured while adding 0.750 mL Pu-238 stock solution to CTMFD solution in order to adjust expected wait time from ~40 seconds to ~10 seconds.

Mass of diluted sample with nalgene and cap (g)	Mass of diluted sample with 0.750 mL stock Pu-238 solution added, nalgene and cap (g)
55.1545	55.7445

Table 26. Mass values measured while adding 0.5 mL UN stock solution to CTMFD solution in order to adjust expected wait time from ~60 seconds to ~10 seconds.

Mass of diluted sample with nalgene and cap (g)	Mass of diluted sample with 0.5 mL stock UN solution added, nalgene and cap (g)
56.1933	56.5888

THIS PAGE INTENTIONALLY LEFT BLANK

LIST OF REFERENCES

[1] Nuclear forces reduced while modernizations continue, says SIPRI (2014, Jun. 16). Stockholm International Peace Research Institute. [Online]. Available: http://www.sipri.org/media/pressreleases/2014/nuclear_May_2014

[2] *Defense Threat Reduction Agency*, DOD Directive 5105.62, Department of Defense, Washington, DC, 2015, pp. 7.

[3] R. Taleyarkhan, J. Lapinskas, B. Archambault, J. Webster, T. Grimes, A. Hagen, K. Fisher, S. McDeavitt, and W. Charlton, "Real-time monitoring of actinides in chemical nuclear fuel reprocessing plants," *Chemical Engineering Research and Design,* vol. 91, no. 4, pp. 688–702, Apr. 2013. doi:10.1016/j.cherd.2013.02.010

[4] J. Lamarsh and A. Baratta, *Introduction to Nuclear Engineering*, 3rd ed. Upper Saddle River: Pearson Education, Inc., 2001, pp. 18–24, 71, 129.

[5] G. F. Knoll, *Radiation Detection and Measurement*, 3rd ed. New York: John Wiley & Sons, Inc., 2000, pp. 3–9, 11–13, 19–20, 73, 223–225, 511.

[6] Radiation Basics (2014, Oct. 17). United States Nuclear Regulatory Commission. [Online]. Available: http://www.nrc.gov/about-nrc/radiation/health-effects/radiation-basics.html

[7] N. Ensslin. (n.d.) The origin of neutron radiation [Online]. Available: http://www.lanl.gov/orgs/n/n1/panda/00326406.pdf. Accessed Apr. 21, 2016.

[8] LS 6500 scintillation system operating manual. (1999, Sep.). Beckman Coulter, Inc. [Online]. Available: http://bti.cornell.edu/wp-content/uploads/2014/04/Beckman_LSC_LS6500manual-2.pdf

[9] E. Bayat, N. Divani-Vais, M. Firoozabadi, and N. Ghal-Eh, "A comparative study on neutron-gamma discrimination with NE213 and UGLLT scintillators using zero-crossing method," *Radiation Physics and Chemistry,* vol. 81, pp. 217–220, Mar. 2012. doi:10.1016/j.radphyschem.2011.10.016

[10] J. Lee and C. Lee, "Response function of NE213 scintillator for 0.5–6 MeV neutrons measured by an improved pulse shape discrimination," *Nuclear Inst. and Methods in Physics Research,* vol. 402, no. 1, pp. 147–154, Jan. 1998. doi:10.1016/S0168–9002(97)01073–5

[11] T. E. Valentine, "Evaluation of prompt fission gamma rays for use in simulating nuclear safeguard measurements," *Annals of Nuclear Energy*, vol. 28, no. 3, pp. 191–201, Feb. 2001. doi:10.1016/S0306–4549(00)00039–6

[12] Nuclear data center at the Korea Atomic Energy Research Institute. Table of Nuclides. [Online]. Available: http://atom.kaeri.re.kr/nuchart/. Accessed Sep. 25, 2015.

[13] P. Frame. (2011, May 10). Boron trifluoride neutron detectors [Online]. Available: https://www.orau.org/ptp/collection/proportional%20counters/bf3info.htm

[14] W. H. Hallenbeck, *Radiation Protection*, Boca Raton: Lewis Publishers, 1994, pp. 58.

[15] B. C. Archambault, J. A. Webster, J. R. Lapinskas, T. F. Grimes, and R. Taleyarkhan, "Development of a novel direction-position sensing fast neutron detector using tensioned metastable fluids," *Nuclear Inst. and Methods in Physics Research A*, vol. 673, pp. 89–97, May 2012. doi:10.1016/j.nima.2011.12.050

INITIAL DISTRIBUTION LIST

1. Defense Technical Information Center
   Ft. Belvoir, Virginia

2. Dudley Knox Library
   Naval Postgraduate School
   Monterey, California